American Journal of Respiratory and Critical Care Medicine/AJRCCM

Resonance as the Mechanism of Daytime Periodic Breathing in Patients with Heart Failure

Journal:	*American Journal of Respiratory And Critical Care Medicine*
Manuscript ID	Blue-201604-0761OC.R1
Manuscript Type:	OC - Original Contribution
Date Submitted by the Author:	n/a
Complete List of Authors:	Sands, Scott; Brigham and Women's Hospital and Harvard Medical School, Division of Sleep Medicine; Monash University, Central Clinical School Mebrate, Yoseph; Imperial College London, International Center for Circulatory Health, National Heart and Lung Institute Edwards, Bradley; Brigham and Women's Hospital and Harvard Medical School, Division of Sleep Medicine, Sleep Disorders Research Division Nemati, Shamim; Brigham and Women\'s Hospital and Harvard Medical School, Division of Sleep Medicine Manisty, Charlotte; University College London, Institute of Cardiovascular Sciences Desai, Akshay; Brigham and Women’s Hospital, Harvard Medical School, Division of Cardiovascular Medicine Wellman, Andrew; Harvard, Medicine Willson, Keith; Imperial College London, International Center for Circulatory Health, National Heart and Lung Institute Francis, Darrel; Imperial College London, International Center for Circulatory Health, National Heart and Lung Institute Butler, James; Brigham and Women\'s Hospital and Harvard Medical School, Division of Sleep Medicine Malhotra, Atul; University of California, San Diego, Division of Pulmonary and Critical Care Medicine
Subject Category:	8.09 Control of Ventilation: Physiology < INTEGRATIVE PHYSIOLOGY AND PATHOLOGY
Keywords:	instability, loop gain, Cheyne-Stokes respiration, heart failure, chemosensitivity

Resonance as the Mechanism of Daytime Periodic Breathing in Patients with Heart Failure

Scott A. Sands[1,2*], Yoseph Mebrate[3,4], Bradley A. Edwards[1,5,6], Shamim Nemati[1], Charlotte H. Manisty[7], Akshay S. Desai[8], Andrew Wellman[1], Keith Willson[3], Darrel P. Francis[3], James P. Butler[1†], Atul Malhotra[1,9†]

[1]Division of Sleep and Circadian Disorders, Brigham and Women's Hospital and Harvard Medical School, Boston, USA;
[2]Department of Allergy, Immunology and Respiratory Medicine and Central Clinical School, The Alfred and Monash University, Melbourne, Australia;
[3]International Center for Circulatory Health, National Heart and Lung Institute, Imperial College London, UK.
[4]Department of Clinical Engineering, Royal Brompton Hospital, London, UK;
[5]Sleep and Circadian Medicine Laboratory, Department of Physiology Monash University, Melbourne, VIC, Australia.
[6]School of Psychological Sciences and Monash Institute of Cognitive and Clinical Neurosciences, Monash University, Melbourne,
[7]Institute of Cardiovascular Sciences, University College London, London UK;
[8]Division of Cardiovascular Medicine, Brigham and Women's Hospital and Harvard Medical School, Boston, USA.
[9]Division of Pulmonary and Critical Care Medicine, University of California San Diego, La Jolla CA, USA.

[†]These authors contributed equally to this work.

[*]Corresponding author: Scott Sands, PhD
Division of Sleep Medicine, Brigham and Women's Hospital,
221 Longwood Ave, Boston 02115, MA, USA.
email: sasands@partners.org | T: +1 8579280341 | F: +1 6177327337

Running title: Mechanism of diurnal periodic breathing

Word count: 3470/3500

Author Contributions. Conception and design: SS, YM, BE, SN, AD, DF, AM. Mathematical framework: SS, SN, JP. Model simulations: SS, YM. Modified approach to assess stability: SS. Data collection and analysis: SS, BE, AW, AM. Drafted the manuscript SS, JB. All authors interpreted data, edited the manuscript for important intellectual content, and approved the final draft.

Support: This study was not supported by industry. Our work was financially supported by the American Heart Association (11POST7360012, 15SDG25890059), National Institute of Health (K24HL093218-01A1, 1R01HL090897-01A2, 5R01HL048531-16, R01HL102321 and P01HL095491), National Health and Medical Research Council of Australia (NHMRC, 1053201), the Menzies Foundation, and the American Thoracic Society Foundation. This work was also supported by Harvard Catalyst (National Center for Research Resources and the National Center for Advancing Translational Sciences, National Institutes of Health Award UL1TR001102). Dr. Sands was also co-investigator on grants from the NHMRC (1038402, 1064163) and NIH (R01HL128658). Dr. Malhotra was PI on NIH R01HL085188, K24HL132105 and co-investigator on R21HL121794, R01HL119201, R01HL081823. As an Officer of the American Thoracic Society, Dr. Malhotra relinquished all outside personal income since 2012. ResMed, Inc. provided a philanthropic donation to the UC San Diego in support of a UCSD sleep center. Dr. Desai reported unrelated grants and personal fees from Novartis, personal fees from St. Jude Medical, Merck, Relypsa, and Janssen. The authors declare no competing financial interests.

At a Glance Commentary

Scientific Knowledge on the Subject: Oscillatory breathing during wakefulness predicts mortality in patients with heart failure but the responsible mechanism is unclear. Associations with increased chemosensitivity and circulatory delay suggest instability of the chemoreflex feedback loop, but oscillatory patterns are often irregular which illustrates that our knowledge is incomplete.

What This Study Adds to the Field: Our study provides the mechanism of daytime ventilatory oscillations in heart failure: Ventilatory oscillations occur due to a chemoreflex resonance or "ringing" effect, whereby a reduced stability (increased loop gain)—due to increased chemosensitivity and delay—paradoxically enhances biological noise as it is propagated around the feedback loop, yielding stronger and more regular oscillations as stability is reduced. Our work may facilitate clinical measurement and interpretation of the oscillatory breathing that precedes sudden death in advanced heart failure.

Abstract

Rationale: In patients with chronic heart failure, daytime oscillatory breathing at rest is associated with high mortality risk. Experimental evidence, including exaggerated ventilatory responses to carbon dioxide (CO_2) and prolonged circulation time, implicates the ventilatory control system and suggests feedback instability (loop gain>1) is responsible. However, daytime oscillatory patterns often appear remarkably irregular versus classical instability (Cheyne-Stokes respiration), suggesting our mechanistic understanding is limited.

Objective: We propose that daytime ventilatory oscillations generally result from a chemoreflex *resonance*, whereby spontaneous biological variations in ventilatory drive repeatedly induce temporary and irregular ringing effects. Importantly, the ease with which spontaneous biological variations induce irregular oscillations (resonance "strength") rises profoundly as loop gain rises towards 1. We test this hypothesis through a comparison of mathematical predictions against actual measurements in patients with heart failure and healthy controls.

Methods: In 25 patients with chronic heart failure and 25 controls, we examined spontaneous oscillations in ventilation and separately quantified loop gain using dynamic inspired CO_2 stimulation.

Measurements and Main Results: Resonance was detected in 24/25 heart failure patients and 18/25 controls. With increased loop gain—consequent to increased chemosensitivity and delay—the strength of spontaneous oscillations increased precipitously as predicted ($r=0.88$), yielding larger ($r=0.78$) and more regular (interpeak interval S.D., $r=-0.68$) oscillations ($p<0.001$ for all, both groups combined).

Conclusions: Our study elucidates the mechanism underlying daytime ventilatory oscillations in heart failure, and provides a means to measure and interpret these oscillations to reveal the underlying chemoreflex hypersensitivity and reduced stability that foretells mortality in this population.

250/250 words

Keywords

instability | loop gain | Cheyne-Stokes respiration | heart failure | chemosensitivity

INTRODUCTION

The presence of daytime ventilatory oscillations is a powerful prognostic indicator of mortality in patients with chronic heart failure, independent of ejection fraction and peak oxygen consumption (1-6), but the underlying pathogenesis remains unclear. The feedback system controlling ventilation is strongly implicated based on evidence that patients with oscillatory ventilation exhibit hypersensitive ventilatory chemoreflexes and increased circulatory delays (5, 7, 8) and evidence that ventilatory oscillations are suppressed by interventions that improve stability (lowered loop gain) namely reducing chemoreflex sensitivity, increasing cardiac output or clamping alveolar carbon dioxide (CO_2) levels (5, 9-13). These findings have led to the prevailing view that feedback instability is responsible (7, 13-16), rather than a central pacemaker (17, 18). Yet there is a broad spectrum of irregular oscillatory patterns observed in patients during wakefulness, many of which differ substantially from the remarkably consistent periodic cycles of apnea and crescendo-decrescendo hyperpnea (Cheyne-Stokes respiration) manifest during sleep and in computer models of feedback instability (16, 19). Thus, an alternative explanation for daytime ventilatory oscillations is needed.

According to prevailing theory, a hypersensitive and delayed ventilatory feedback system will yield ventilatory oscillations when the critical tipping-point for instability is exceeded (loop gain >1), but when the system is fundamentally stable oscillations should be damped away (loop gain <1, see Methods—Theory and Online Supplement Fig. E1-2) (7, 14, 16, 20). Yet the instability theory has a critical weakness that precludes its general applicability: Even stable feedback systems (loop gain <1) manifest a *resonance* or "ringing" effect whereby random biological disturbances (e.g. intrinsic neural variability, sighs, and behavioral effects) repeatedly disturb the feedback loop, promoting temporary overshoot and undershoot oscillations with imprecise timing and amplitude (21-24). We propose that this concept underlies the pathogenesis of daytime ventilatory oscillations in patients with heart failure.

Here we assess whether ventilatory oscillations that occur during wakefulness are the consequence of a resonance in the chemoreflex feedback loop regulating ventilation. First we describe and illustrate the concept of resonance as applicable to ventilatory oscillations. Subsequently, we assess daytime ventilatory oscillations in patients with heart failure and controls to test the hypothesis that the oscillatory behavior depends precisely on the stability (loop gain) of the ventilatory chemoreflex system (see Methods—Theory). Concordance with theory is taken to support chemoreflex resonance as the mechanism responsible. Preliminary data have been presented in abstract form (25).

METHODS

Theoretical Basis of Resonance

The concepts of loop gain (i.e. stability) and resonance are well established, but the concept that loop gain precisely determines the strength of the resonance and the ensuing oscillatory nature of breathing under normal (stable) conditions has not been detailed previously (see Online Supplement for details).

The stability of the chemoreflex feedback loop is determined by its *loop gain,* the ratio of the compensatory ventilatory feedback response that opposes a ventilatory disturbance (see conceptual model, Fig. 1A). An isolated ventilatory disturbance provided to a stable system (loop gain = 0.8; Fig. 1B) yields a oscillatory "ringing" effect at a particular frequency before gradually damping out. Yet an ongoing disturbance at this frequency (akin to a child being pushed on a swing) produces ventilatory fluctuations that are considerably larger than the disturbance itself (Fig. 1C). The ease by which ventilation fluctuates as a result of a disturbance (26-30) is determined by loop gain according to:

$$T = 1/(1-\textit{loop gain}) \qquad \text{(Equation 1)}$$

where T defines the strength of the resonance and the strength of the ensuing oscillations. As loop gain rises towards 1 (i.e. the threshold for instability), feedback profoundly amplifies disturbances: For example, for a loop gain of 0.5, disturbances are doubled by the feedback system (T=2); when loop gain is 0.8, disturbances are 5-fold greater than they would have been without feedback (T=5, Fig. 1C)

Simulated ventilatory oscillations. To illustrate the oscillatory characteristics that occur in the presence of spontaneous biological variations or "noise" (31), we examined a simple model system at various levels of loop gain (Fig. 2). Note the distinct emergence of irregular oscillatory patterns (Fig. 2A) that bare a remarkable resemblance to ventilatory patterns observed in heart failure (13, 32, 33) and controls with experimentally-raised loop gain (34) (see Results).

Importantly, we now recognize that as loop gain rises, a stronger resonance occurs that can be quantitatively identified as a stronger peak in the power spectrum of ventilation (Fig. 2B), ultimately yielding larger and more regular oscillations.

Methodological Approach

Our primary objective was to test whether oscillatory strength—namely amplitude relative to biological noise (i.e. T)—is uniquely related to the loop gain of the ventilatory control system according to Equation 1. Loop gain was measured separately using dynamic inspired CO_2 (see below) during wakefulness. We also assessed whether larger amplitude, more regular oscillations are associated with a higher loop gain, and whether the spectral profile of oscillations matches that expected of a resonance.

Participants

Twenty-five patients with an established clinical diagnosis of chronic heart failure (any left ventricular ejection fraction) and twenty-five controls without heart failure were studied. Participants attended as part of larger ongoing prospective studies investigating the stabilizing mechanisms of acetazolamide and oxygen and the causes of sleep apnea (interventions were not given before/during this study). Inclusion required the absence of severe comorbidities including lung, kidney and liver diseases. Participants taking medications affecting respiratory control (including opioids, benzodiazepines, barbiturates, acetazolamide, theophylline, indomethacin, pseudoephedrine) were excluded. Participants provided written informed consent and approval was granted by the Partners' Institutional Review Board. Details are provided in the Online Supplement.

Procedure

Participants were examined by a physician before study procedures. Measures were made in the morning (7am-12pm) to minimize potential time of day effects. Participants were instrumented with a sealed nasal mask to facilitate measurement of ventilation (heated pneumotachograph and pressure transducer; Hans-Rudolph Model 3700, Kansas City, MO, USA; Validyne Engineering Corp., Model MP45-14-871, Northridge, CA, USA; ventilation = tidal volume × respiratory rate). Absence of mask leak was confirmed by forced expiration against a closed exhalation port. A thin catheter was placed through a port in the mask to measure intranasal CO_2 tension (PCO_2; Vacumetrics Inc., Model 17625, Ventura, CA, USA) enabling assessment of inspired PCO_2 and end-tidal PCO_2 (a surrogate for alveolar and arterial PCO_2). Electroencephalography (C3-A2, O2-A1) was performed to document wakefulness. Participants lay supine, and were instructed to relax, keep their eyes open and mouth closed (confirmed via visual assessment) and watched television as a distraction. Ventilation was recorded without interruption for 20 min to assess spontaneous ventilatory oscillations (see below). Participants were subsequently connected to a non-rebreathing circuit for measurement of their chemoreflex stability (i.e. loop gain) using inspired CO_2. For each procedure, a period of acclimation was provided to ensure ventilation and end-tidal PCO_2 settled to an equilibrium before proceeding. Signals were sampled at 125 Hz (Power 1401 and Spike2, Cambridge Electronic Design Limited, Cambridge, UK); breath-by-breath respiratory signals were resampled at 4 Hz for further analyses.

Ventilatory Oscillations

To quantify the oscillatory nature of ventilation during spontaneous breathing, we performed spectral analysis and fit a physiological equation that describes the spectral profile of a resonance (Fig. 2B; one-compartment delayed feedback stimulated by noise, see Online Supplement). This analysis revealed a single parameter, T, a measure of the oscillatory strength (amplitude / background noise) that is theoretically related

to loop gain (Equation 1). The peak-to-peak amplitude and irregularity (interpeak interval S.D.) of ventilatory oscillations were also quantified (see Online Supplement).

Chemoreflex Stability

Loop gain was quantified using dynamic inspired CO_2 stimulation using a modified method employing pulsatile CO_2 stimuli. 7% inspired CO_2 was administered for a duration of 0.5 min, every 3 min for a total of 30 min (10 pulses) that has the equivalent effect of stimulating ventilation at 5 frequencies simultaneously (0.33, 0.67, 1, 1.33, 1.67 cycles/min). Chemosensitivity (Δventilation/Δalveolar PCO_2), CO_2 damping or *plant gain* (Δalveolar PCO_2/Δventilation) and accompanying delays were calculated at each frequency to determine loop gain (chemosensivity×plant gain, see Online Supplement).

Statistics

Linear regression assessed the relationship between the oscillatory strength (T, spectral analysis) and the underlying loop gain (CO_2 stimulation). Oscillatory strength was first transformed ($1-1/T$, reflecting the estimated loop gain) before statistical analysis; transformed data became normally distributed and correlations with putative physiological determinants became linear, as expected by theory. Fisher F-tests compared the resonance model of the power spectrum versus the biological noise model without resonance within individuals; a significant improvement over noise confirmed the presence of a resonance (i.e. T significantly >1). Student's t-tests compared variables between heart failure and controls; general linear models compared variables adjusted for age, sex, and BMI (see Online Supplement for matched comparisons). Determinants of loop gain, including chemoreflex sensitivity and delay, were quantified at a common frequency (1 cycle/min) for regression analyses; multiple regression results were summarized by presenting the improvement in the model r^2 with the inclusion of each determinant in a sequential manner (forward stepwise). Unless specified otherwise, *loop gain* refers to the value at the natural frequency. Statistical significance was accepted at $p<0.05$.

RESULTS

Characteristics

Participant characteristics are detailed in Table 1. The heart failure population exhibited a range of severities of left ventricular ejection fraction (ejection fraction range: 15-67%; two individuals had preserved ejection fraction). All heart failure patients were on optimal medical therapy per attending cardiologist.

Chemoreflex Stability

Assessment of chemoreflex feedback control of ventilation is detailed in Table 2. Patients with heart failure exhibited stable ventilatory control systems during wakefulness (loop gain range: 0.10-0.84) and exhibited a 71% higher loop gain than controls ($p=0.003$, adjusted for age, sex, BMI).

Ventilatory Oscillations

Example traces. Ventilatory patterns during spontaneous breathing in 5 patients with heart failure are shown in Fig. 3A. Note the profound, irregular oscillations bear a remarkable resemblance to the ventilatory oscillations emerging from feedback amplification of 1/*f* noise (Fig. 3A versus Fig. 2A).

Resonance model. The resonance model closely fit the measured spectral profile of ventilatory oscillations for each participant (see examples in Fig 3B and summary data in Table 3). The presence of a significant resonance was observed in 24/25 patients with heart failure and 18/25 controls (Fisher F-test, comparing resonance to biological noise without feedback). Participants without a significant resonance (ventilatory variability resembled noise) tended to have a lower loop gain (see Online Supplement).

We observed a notable concordance between the oscillatory strength (T) seen using spectral analysis and the underlying loop gain taken from CO_2 stimulation (Fig. 4A), as expected from theory (Equation 1). That is, the underlying loop gain accurately explains the oscillatory nature of ventilation. Importantly, this association enabled loop gain to be estimated accurately from spontaneous oscillations (estimated loop gain = $1-1/T$; Fig. 4A).

Consistent with prediction, increasing loop gain was associated with oscillations that were larger (Fig. 4B) and had less irregular timing (smaller S.D. of interpeak interval, Fig. 4C).

The period of spontaneous oscillations was also associated with the measured natural cycling period (1/[natural frequency] based on CO_2 stimulation, $r=0.75$, $p<0.001$) consistent with feedback resonance.

Determinants of Reduced Stability and Oscillations

Linear regression models included the four loop gain determinants shown in Table 2.

Determinants of chemoreflex stability. Across all participants, increased loop gain was explained by an increase in chemoreflex sensitivity (univariate $r^2=0.42$, $p<0.001$), chemoreflex delay (univariate $r^2=0.14$;

multiple regression Δr^2=0.24, p<0.001), and plant gain (i.e. reduced lung volume; univariate r^2<0.01; multiple regression Δr^2=0.13, p<0.001).

Determinants of ventilatory oscillations. A stronger resonance (T, spectral analysis) was associated with increased chemoreflex sensitivity (univariate r^2=0.36, p<0.001), plant gain (univariate r^2<0.01; multiple regression Δr^2=0.15, p<0.001) and circulatory delay (univariate r^2=0.07; multiple regression Δr^2=0.14, p<0.001). The presence/absence of heart failure explained a minor additional component (Δr^2=0.03, p<0.001) suggesting that factors relating to heart failure beyond the determinants reported had a minor independent impact. Oscillatory amplitude and irregularity were also explained by chemoreflex sensitivity and delays (Online Supplement).

DISCUSSION

Our study elucidates the mechanism underlying daytime ventilatory oscillations, a key predictor of mortality in patients with heart failure (1-6). We found that reduced stability (increased loop gain)—consequent to increased chemosensitivity, delay and plant gain—yields stronger oscillations precisely as expected based on the theoretical concept of resonance (Equation 1). Specifically, the chemoreflex feedback system regulating ventilation paradoxically enhances biological noise near the frequency of periodic breathing, to yield overshoot and undershoot ventilatory oscillations. These ventilatory oscillations in heart failure are typically irregular (Fig. 3A), and conform to a model of feedback resonance in 96% of patients (Fig. 3B). As loop gain rises towards 1, oscillations become larger and more regular (Figs. 2 and 4), yielding prominent periodic breathing despite being classed as a 'stable system' according to classical criteria (loop gain<1). In contrast with current understanding, the more extreme conditions of feedback instability are therefore not necessary for ventilatory oscillations to occur in heart failure (7, 13-16). Overall, our data are remarkably consistent with chemoreflex resonance as the predominant mechanism responsible. Our work therefore provides the field with a validated framework for interpreting and quantifying the broad range of oscillatory ventilatory behaviors seen commonly in patients with heart failure.

Comparison with Available Evidence

By linking the clinical pattern of ventilatory oscillations to the function of the chemoreflex feedback system that regulates ventilation, we provide a unifying explanation for a host of previous empirical findings. Observational studies consistently demonstrate associations between daytime oscillatory breathing in heart failure and factors that promote a less stable feedback regulation of ventilation, namely increased chemosensitivity and circulatory delay (7, 8, 12). Interventions that diminish feedback act to suppress oscillations, seen as a reduced variability and the disappearance of a peak in the power spectrum of ventilation (5, 9-11, 13). In healthy subjects and animals breathing spontaneously, experimental studies have demonstrated associations between ventilatory fluctuations and prior swings in ventilation and PCO_2, which are dependent on intact chemosensitivity (22, 26, 35). Modeling studies have also suggested that a stronger chemoreflex response or higher loop gain yields quasi-oscillations in the presence of biological noise (24), although a quantitative relationship between oscillatory behavior and reduced stability had not been proposed or tested experimentally until now. Taken together with the current study, the available evidence now overwhelmingly implicates chemoreflex feedback regulation in the ventilatory oscillations observed.

Physiological Insights

Our study experimentally links the nature of ventilatory oscillations to the underlying structure of the chemoreflex control system regulating ventilation. Several key insights can be drawn from our work:

Based on the concept of resonance, some degree of ventilatory oscillations must occur as a necessary side-effect of homeostatic regulation. Specifically, a greater chemoreflex sensitivity will more completely suppress a long-term or steady-state disturbance to ventilation (e.g. a change in respiratory mechanics or metabolic rate), but will yield a greater amplification of biological noise at its characteristic frequency (see Fig. 2B, see also Online Supplement). The greater circulatory delay that occurs in heart failure will increase the amplification at the resonance, but also moves the resonance to a lower frequency where biological noise is greater.

Oscillations result from chemoreflex feedback across a stability-instability continuum. Individuals with very low loop gain (e.g. 0<loop gain≤0.25) exhibit a pattern resembling biological noise. Those with normal loop gain (0.25<loop gain≤0.5) exhibit weak and irregular oscillations. Patients with elevated loop gain (0.5<loop gain≤1) manifest stronger and more regular oscillations (Fig. 3). Finally, consistent periodic breathing occurs in the most extreme cases when the threshold for instability is breached (loop gain>1).

When loop gain is below 1, the magnitude of biological noise plays a key role in the pathogenesis of oscillatory breathing. For example, patients i and iii have quite similar loop gains but patient i has 2-fold larger oscillations due to increased noise (see Figs. 2 and 3). Consequently, ventilatory fluctuations can be larger as a consequence of increased loop gain or increased noise. Thus, two distinct phenotypes of excessive ventilatory variability can be described: those driven largely by hypersensitive chemoreflex feedback (normal biological noise levels) and those with increased biological noise i.e. ataxic opioid-induced ventilatory fluctuations (36) or ventilatory fluctuations in rapid-eye movement sleep (37).

The concept of resonance has important implications for periodic breathing during sleep, known as central sleep apnea, which is also a strong prognostic marker of mortality in heart failure (1). Although sleep diminishes chemosensitivity *per se*, ventilatory oscillations become even more prominent (9). Key contributing factors include changes to state (sleep-wake transitions, arousals) and upper-airway patency (e.g. swings in dilator muscle tone) (38). Insofar as arousals and changes to upper-airway patency are tied to PCO_2, such effects effectively raise loop gain by exacerbating changes in ventilation per change in PCO_2. However, to the extent that arousals and upper airway effects are random, they provide an additional source of biological variability that will act to promote oscillatory breathing with maximum impact in those with elevated loop gain. Diminishing these disturbances with hypnotics/CPAP can indeed improve central sleep apnea (39). Such disturbances may also explain residual events after loop gain is lowered to stable levels with intervention (40).

The concept also has implications for obstructive sleep apnea, a condition characterized by irregular ventilatory oscillations due to a combination of increased upper airway collapsibility and reduced ventilatory stability (41). Interestingly, reducing loop gain can improve obstructive sleep apnea severity even when the

control system is strictly stable before intervention (41), potentially due to damping of chemoreflex resonance effects.

Clinical Implications

In patients with heart failure, increased chemosensitivity and consequent ventilatory oscillations are harbingers of the neurohumoral derangement that ultimately predisposes to mortality (42, 43). On this basis, a simple means to quantify reduced stability, as distinct from increased biological noise, may have clinical utility. Importantly, the current work enables a quantitative identification of the propensity to instability in individual patients from spontaneous breathing, without intervention. We and others have used spontaneous breathing to quantify stability (26, 41, 44, 45), but the use of a single variable to estimate stability without intervention has not been validated to date. Our approach may help 1.) recognize the predisposition to Cheyne-Stokes respiration during wakefulness or sleep, 2.) provide a means to titrate medications or screen those at high risk of sudden cardiac death, 3.) assess the impact of novel therapies designed to reduce chemosensitivity. However, further investigation is warranted.

Limitations

Detailed mechanisms. Our study does not attempt to elucidate the specific chemoreceptors responsible for the ventilatory oscillations observed. Peripheral and central chemoreceptor systems may both contribute to the dynamic response measured with CO_2 stimulation, although available evidence suggests an essential role for the carotid body chemoreceptors in the ventilatory oscillations and mortality in heart failure (46-49). Hypoxic chemosensitivity may also play a role (8), so including it in a measure of loop gain may further improve the associations observed. We also did not seek to elucidate the main source of ventilatory noise. Sources may be either extrinsic (e.g. behavioral inputs, neural variability external to chemoreflex feedback) or intrinsic (e.g. neural variability at the level of respiratory pattern generator or within chemoreceptor circuits in the medulla). The precise details of ventilatory disturbances were not under investigation: the essential point is that biological variability acts to disturb ventilation across a broad frequency range in all individuals.

End-tidal PCO_2 as an estimate of alveolar and arterial PCO_2. End-tidal PCO_2 is used ubiquitously in ventilatory control studies of patients with and without heart failure to reflect breath-to-breath changes to alveolar and arterial PCO_2. We note that particular care was taken to ensure a sufficient plateau such that end-tidal PCO_2 reflected alveolar levels (see Online Supplement). Moreover, we excluded patients with lung disease; nonetheless, the difference between end-tidal and arterial PCO_2 may be considerable in some patients with heart failure (e.g. via subclinical pulmonary congestion). We note, however, that a constant discrepancy between these two variables will have no impact on the values of loop gain measured as this calculation depends on relative PCO_2 changes rather than the absolute value.

Non-linearities. The resonance concept employed here can be considered a linear simplification of more general nonlinear behavior. We note that spectral analysis of the oscillation traces revealed subtle higher harmonics at multiples of the natural frequency (i.e. not explained by the linear resonance model) in 3/25 patients with heart failure and 0/25 controls, consistent with the absence of nonlinear effects except in extreme cases (see patients ii and iv in Fig. 3, note smaller peaks not explained by the red model trace; see Online Supplement).

Conclusions

Using a combination of mathematical modeling and direct measurement in patients with heart failure, our study demonstrates that daytime breathing oscillations in heart failure are readily explained by a potent resonance or "ringing" effect due to the chemoreflex feedback system regulating ventilation. Reduced stability—consequent to increased chemosensitivity and delay—leads to a greater amplification and propagation of biological noise around the feedback loop, yielding transient overshoot and undershoot oscillations that become profound as stability is reduced. We may now decipher oscillatory characteristics to more readily detect and interpret the otherwise covert increases in chemoreflex sensitivity that are known to occur with advanced heart failure and foretell mortality.

Acknowledgements

The authors are grateful for the technical assistance from Alison Foster, Lauren Hess, Pamela DeYoung and Erik Smales, for the medical assessments performed by Drs. Robert Owens, David McSharry, and Jeremy Beitler, for the facilitation of patient recruitment from Drs. Michael Givertz, James Januzzi, Anju Nohria, William Dec, Garrick Stewart, Eldrin Lewis, Leonard Lilly, Lynne Stevenson and for discussions with Drs. Tilo Winkler and Morgan Mitchell.

References

1. Lanfranchi PA, Braghiroli A, Bosimini E, Mazzuero G, Colombo R, Donner CF, Giannuzzi P. Prognostic value of nocturnal cheyne-stokes respiration in chronic heart failure. *Circulation* 1999;99:1435-1440.
2. Corra U, Pistono M, Mezzani A, Braghiroli A, Giordano A, Lanfranchi P, Bosimini E, Gnemmi M, Giannuzzi P. Sleep and exertional periodic breathing in chronic heart failure: Prognostic importance and interdependence. *Circulation* 2006;113:44-50.
3. Guazzi M, Raimondo R, Vicenzi M, Arena R, Proserpio C, Sarzi Braga S, Pedretti R. Exercise oscillatory ventilation may predict sudden cardiac death in heart failure patients. *J Am Coll Cardiol* 2007;50:299-308.
4. Arena R, Myers J, Abella J, Peberdy MA, Pinkstaff S, Bensimhon D, Chase P, Guazzi M. Prognostic value of timing and duration characteristics of exercise oscillatory ventilation in patients with heart failure. *J Heart Lung Transplant* 2008;27:341-347.
5. Ponikowski P, Anker SD, Chua TP, Francis D, Banasiak W, Poole-Wilson PA, Coats AJ, Piepoli M. Oscillatory breathing patterns during wakefulness in patients with chronic heart failure: Clinical implications and role of augmented peripheral chemosensitivity. *Circulation* 1999;100:2418-2424.
6. Brack T, Thuer I, Clarenbach CF, Senn O, Noll G, Russi EW, Bloch KE. Daytime cheyne-stokes respiration in ambulatory patients with severe congestive heart failure is associated with increased mortality. *Chest* 2007;132:1463-1471.
7. Francis DP, Willson K, Davies LC, Coats AJ, Piepoli M. Quantitative general theory for periodic breathing in chronic heart failure and its clinical implications. *Circulation* 2000;102:2214-2221.
8. Giannoni A, Emdin M, Poletti R, Bramanti F, Prontera C, Piepoli M, Passino C. Clinical significance of chemosensitivity in chronic heart failure: Influence on neurohormonal derangement, cheyne-stokes respiration and arrhythmias. *Clin Sci (Lond)* 2008;114:489-497.
9. Fontana M, Emdin M, Giannoni A, Iudice G, Baruah R, Passino C. Effect of acetazolamide on chemosensitivity, cheyne-stokes respiration, and response to effort in patients with heart failure. *Am J Cardiol* 2011;107:1675-1680.
10. Murphy RM, Shah RV, Malhotra R, Pappagianopoulos PP, Hough SS, Systrom DM, Semigran MJ, Lewis GD. Exercise oscillatory ventilation in systolic heart failure: An indicator of impaired hemodynamic response to exercise. *Circulation* 2011;124:1442-1451.
11. Giannoni A, Baruah R, Willson K, Mebrate Y, Mayet J, Emdin M, Hughes AD, Manisty CH, Francis DP. Real-time dynamic carbon dioxide administration: A novel treatment strategy for stabilization of periodic breathing with potential application to central sleep apnea. *J Am Coll Cardiol* 2010;56:1832-1837.
12. Mortara A, Sleight P, Pinna GD, Maestri R, Capomolla S, Febo O, La Rovere MT, Cobelli F. Association between hemodynamic impairment and cheyne-stokes respiration and periodic breathing in chronic stable congestive heart failure secondary to ischemic or idiopathic dilated cardiomyopathy. *Am J Cardiol* 1999;84:900-904.
13. Pinna GD, Maestri R, Mortara A, La Rovere MT, Fanfulla F, Sleight P. Periodic breathing in heart failure patients: Testing the hypothesis of instability of the chemoreflex loop. *J Appl Physiol* 2000;89:2147-2157.
14. Khoo MC, Kronauer RE, Strohl KP, Slutsky AS. Factors inducing periodic breathing in humans: A general model. *J Appl Physiol* 1982;53:644-659.
15. Cherniack NS, Longobardo GS. Cheyne-stokes breathing. An instability in physiologic control. *N Engl J Med* 1973;288:952-957.
16. Sands SA, Edwards BA, Kee K, Turton A, Skuza EM, Roebuck T, O'Driscoll DM, Hamilton GS, Naughton MT, Berger PJ. Loop gain as a means to predict a positive airway pressure suppression of cheyne-stokes respiration in patients with heart failure. *Am J Respir Crit Care Med* 2011;184:1067-1075.
17. Franklin KA, Sandstrom E, Johansson G, Balfors EM. Hemodynamics, cerebral circulation, and oxygen saturation in cheyne-stokes respiration. *J Appl Physiol* 1997;83:1184-1191.
18. Bartsch S, Haouzi P. Periodic breathing with no heart beat. *Chest* 2013;144:1378-1380.
19. Milhorn HT, Guyton AC. An analog computer analysis of cheyne-stokes breathing. *Journal of Applied Physiology* 1965;20:328-333.
20. Nyquist H. Regeneration theory. *Bell System Technical Journal* 1932;11:126-147.
21. Khoo MCK. Complex dynamics in physiological control systems. In: Herrick RJ, editor. Physiological control systems analysis, simulation, and estimation. New Jersey: John Wiley & Sons, Inc.; 2000. p. 271-308.
22. Van den Aardweg JG, Karemaker JM. Influence of chemoreflexes on respiratory variability in healthy subjects. *Am J Respir Crit Care Med* 2002;165:1041-1047.
23. Modarreszadeh M, Bruce EN. Ventilatory variability induced by spontaneous variations of paco2 in humans. *J Appl Physiol* 1994;76:2765-2775.
24. Khoo MC. Determinants of ventilatory instability and variability. *Respir Physiol* 2000;122:167-182.
25. Sands SA, Nemati S, Mebrate Y, Edwards BA, Manisty CH, Turton A, Wellman A, Willson K, Francis DP, Malhotra A. Ventilatory oscillations in stable control systems as an interaction between external disturbances and feedback stability [abstract]. *SLEEP* 2012;35:A48.
26. Nemati S, Edwards BA, Sands SA, Berger PJ, Wellman A, Verghese GC, Malhotra A, Butler JP. Model-based characterization of ventilatory stability using spontaneous breathing. *J Appl Physiol* 2011;111:55-67.
27. Hammer PE, Saul JP. Resonance in a mathematical model of baroreflex control: Arterial blood pressure waves accompanying postural stress. *Am J Physiol Regul Integr Comp Physiol* 2005;288:R1637-1648.
28. Nisbet RM, Gurney WSC. A simple mechanism for population cycles. *Nature* 1976;263:319-320.
29. Ogata K. Frequency response analysis. In: Robbins T, editor. Modern control engineering, 3rd ed. New Jersey: Prentice-Hall, Inc.; 1997. p. 471-608.
30. Bode H. Network analysis and feedback filter design. New York, NY: D. Van Nostrand Company; 1945.
31. Mutch WA, Harms S, Ruth Graham M, Kowalski SE, Girling LG, Lefevre GR. Biologically variable or naturally noisy mechanical ventilation recruits atelectatic lung. *Am J Respir Crit Care Med* 2000;162:319-323.
32. Garde A, Sornmo L, Jane R, Giraldo BF. Breathing pattern characterization in chronic heart failure patients using the respiratory flow signal. *Ann Biomed Eng* 2010;38:3572-3580.
33. Mortara A, Sleight P, Pinna GD, Maestri R, Prpa A, La Rovere MT, Cobelli F, Tavazzi L. Abnormal awake respiratory patterns are common in chronic heart failure and may prevent evaluation of autonomic tone by measures of heart rate variability. *Circulation* 1997;96:246-252.
34. Wellman A, Malhotra A, Fogel RB, Edwards JK, Schory K, White DP. Respiratory system loop gain in normal men and women measured with proportional-assist ventilation. *J Appl Physiol* 2003;94:205-212.
35. Khatib MF, Oku Y, Bruce EN. Contribution of chemical feedback loops to breath-to-breath variability of tidal volume. *Respir Physiol* 1991;83:115-127.
36. Farney RJ, Walker JM, Cloward TV, Rhondeau S. Sleep-disordered breathing associated with long-term opioid therapy. *Chest* 2003;123:632-639.
37. Rostig S, Kantelhardt JW, Penzel T, Cassel W, Peter JH, Vogelmeier C, Becker HF, Jerrentrup A. Nonrandom variability of respiration during sleep in healthy humans. *Sleep* 2005;28:411-417.

38. Pinna GD, Robbi E, Pizza F, Caporotondi A, La Rovere MT, Maestri R. Sleep-wake fluctuations and respiratory events during cheyne-stokes respiration in patients with heart failure. *J Sleep Res* 2014;23:347-357.
39. Quadri S, Drake C, Hudgel DW. Improvement of idiopathic central sleep apnea with zolpidem. *J Clin Sleep Med* 2009;5:122-129.
40. Sands SA, Edwards BA, Kee K, Stuart-Andrews CR, Skuza EM, Roebuck T, Turton A, Hamilton GS, Naughton MT, Berger PJ. Control theory prediction of resolved cheyne-stokes respiration in heart failure. *European Respiratory Journal* 2016;In Press.
41. Terrill PI, Edwards BA, Nemati S, Butler JP, Owens RL, Eckert DJ, White DP, Malhotra A, Wellman A, Sands SA. Quantifying the ventilatory control contribution to sleep apnoea using polysomnography. *Eur Respir J* 2015;45:408-418.
42. Giannoni A, Emdin M, Bramanti F, Iudice G, Francis DP, Barsotti A, Piepoli M, Passino C. Combined increased chemosensitivity to hypoxia and hypercapnia as a prognosticator in heart failure. *J Am Coll Cardiol* 2009;53:1975-1980.
43. Ponikowski P, Chua TP, Anker SD, Francis DP, Doehner W, Banasiak W, Poole-Wilson PA, Piepoli MF, Coats AJ. Peripheral chemoreceptor hypersensitivity: An ominous sign in patients with chronic heart failure. *Circulation* 2001;104:544-549.
44. Asyali MH, Berry RB, Khoo MC. Assessment of closed-loop ventilatory stability in obstructive sleep apnea. *IEEE Trans Biomed Eng* 2002;49:206-216.
45. Fleming PJ, Goncalves AL, Levine MR, Woollard S. The development of stability of respiration in human infants: Changes in ventilatory responses to spontaneous sighs. *J Physiol* 1984;347:1-16.
46. Khoo MC, Yang F, Shin JJ, Westbrook PR. Estimation of dynamic chemoresponsiveness in wakefulness and non-rapid-eye-movement sleep. *J Appl Physiol* 1995;78:1052-1064.
47. Del Rio R, Marcus NJ, Schultz HD. Carotid chemoreceptor ablation improves survival in heart failure: Rescuing autonomic control of cardiorespiratory function. *J Am Coll Cardiol* 2013;62:2422-2430.
48. Niewinski P, Janczak D, Rucinski A, Jazwiec P, Sobotka PA, Engelman ZJ, Fudim M, Tubek S, Jankowska EA, Banasiak W, Hart EC, Paton JF, Ponikowski P. Carotid body removal for treatment of chronic systolic heart failure. *International journal of cardiology* 2013;168:2506-2509.
49. Solin P, Roebuck T, Johns DP, Walters EH, Naughton MT. Peripheral and central ventilatory responses in central sleep apnea with and without congestive heart failure. *Am J Respir Crit Care Med* 2000;162:2194-2200.
50. Wellman A, Eckert DJ, Jordan AS, Edwards BA, Passaglia CL, Jackson AC, Gautam S, Owens RL, Malhotra A, White DP. A method for measuring and modeling the physiological traits causing obstructive sleep apnea. *J Appl Physiol* 2011;110:1627-1637.

TABLES

Table 1: Patient Characteristics

Characteristics	Heart failure N=25	Controls N=25
Male:Female	23:2	15:10†
Age, years	61±13	53±13
Body mass index (kg/m^2)	31±7	32±7
Systolic dysfunction (Y:N)	23:2	-
Left-ventricular ejection fraction (%)	38±15	60±3‡§
New York Heart Association class (I:II:III), N	3:13:8	-
Medications, N (%)		
Beta-blockers	24 (96)	0 (0)†
Loop diuretics	17 (68)	0 (0)†
ACEi or AT2R blockers	23 (92)	2 (8)†
Spironolactone	9 (36)	0 (0)†
Digoxin	6 (24)	0 (0)†

Values are mean±S.D. †$p<0.05$ (Fisher exact test). ‡Measured in a subset of 5/26 controls (and all participants with heart failure). §$p<0.001$ heart failure vs. controls (Student's t-test). ACEi=angiotensin-converting enzyme inhibitor. AT2R=angiotensin type II receptor.

Table 2. Chemoreflex stability

Characteristics	Heart failure N=25	Controls N=25
Summary		
Loop gain	0.43±0.21 (range: 0.10-0.84)	0.25±0.09*** (range: 0.06-0.45)
Natural frequency (cycles/min)	1.33±0.39 (range: 0.78-2.57)	1.85±0.51*** (range: 1.15-2.63)
Loop gain determinants‡:		
Chemoreflex sensitivity (L/min/mmHg)§	0.59±0.24	0.48±0.20†
Plant gain (mmHg/L.min)§	0.89±0.21	0.99±0.23
Chemoreflex delay (s)‖	18.2±4.6	13.8±3.3**
Plant delay (s)‖	7.9±1.4	8.2±1.6

Values are mean±S.D. **$p<0.01$, ***$p<0.001$ heart failure versus controls. †Non-significant trend ($p=0.08$). ‡Values are reported for 1 cycle/min oscillations. §Chemoreflex sensitivity or *controller gain* describes the change in ventilation in response to a 1 mmHg oscillation in alveolar PCO_2. Plant gain describes the change in alveolar PCO_2 caused by a 1 L/min oscillation in ventilation. ‖Chemoreflex delay describes the phase shift between alveolar PCO_2 and ventilation (delay = phase lag / 360° × 60) (7). This value reflects the lung-to-chemoreceptor circulation time plus additional time lags due to mixing of CO_2 in the blood and tissues. Likewise, plant delay describes the phase shift between ventilation and alveolar PCO_2 due to CO_2 mixing in the lungs. Values are presented in units of time rather than phase to facilitate interpretation.

Table 3. Ventilatory oscillations

Characteristics	Heart failure N=25	Controls N=25
Power spectral analysis of feedback amplification*		
Oscillatory strength, T	1.7 [1.2] (range: 1.2-11.3)	1.4 [0.2]††† (range: 1.1-2.4)
Estimated loop gain, 1−1/T	0.46±0.19	0.29±0.11†††
Estimated natural frequency (cycles/min)	1.7±0.5	2.5±0.6†††
Significant resonance detected‡ (Y:N)	24:1	18:7§
Time-domain analysis		
Amplitude (%mean)	47 [44]	34 [23]†
Inter-peak interval S.D. (%mean)	26±8	33±6††

Values are mean±S.D. or median[75th minus 25th percentile]. *A resonance model was fit to the ventilation power spectrum to summarize the data. The general model is given by $y=S_d(f)/|1-LG(f)|^2$ where the noise component $S_d(f)$ is assumed to conform to a power law ($S_d(f)=\beta f^{-\alpha}$ where α=exponent, β=offset, f=frequency) and the chemoreflex influence is described by the simplest possible model ($LG(f)=-ke^{-i2\pi f\delta}/(1+i2\pi f\tau)$ where k=gain, τ=time-constant, δ=delay) (41, 50). †p<0.05, ††p<0.01, †††p<0.001. ‡Fisher F-test compared the resonance model (feedback stimulated by biological noise) to noise (without feedback) for each individual. §p<0.05 Fisher exact test.

Figure Legends

Figure 1. Concept of chemoreflex resonance and the relationship with loop gain. (**A**) Feedback model for the chemoreflex regulation of ventilation. (**B**) In a stable system, a temporary disturbance that raises ventilation—thereby lowering alveolar CO_2 and later eliciting a reflex reduction in ventilatory drive—ultimately yields a resonance or "ringing" effect characterized by successive overshoot/undershoot fluctuations that damp out over time. Note that each feedback response (overshoot/undershoot) is ~0.8 times smaller than the prior deflection in ventilation (loop gain = 0.8). (**C**) In the same system, an ongoing disturbance is amplified to yield 5-fold swings in ventilation even though feedback is stable (T=5, see Equation 1).

Figure 2. Simulated chemoreflex oscillations. (**A**) A biological disturbance (top signal) is applied to ventilation for chemoreflex systems with increasing loop gain (reduced stability). Tidal breaths are drawn to faciliate comparison with ventilatory oscillations seen in patients with heart failure. (**B**) Spectral view of signals in panel **A** illustrates how biological noise is amplified by the system in a particular range of frequencies (near 1 cycle/min). In theory, the strength of the oscillation (T = amplitude / noise, vertical arrows) at the frequency of periodic breathing ("natural" cycle frequency), is determined by loop gain (Equation 1). Note also that slower disturbances are inhibited (reduced power at lower frequencies) as expected of homeostatic feedback (see Online Supplement).

Figure 3. Daytime ventilatory oscillations in patients with heart failure. (**A**) Ventilation data from 5 patients (i-v) are shown superimposed on ventilatory flow waveforms. (**B**) Corresponding power spectra are shown. Note the close fit of the resonance model (red lines, shading denotes S.E.M.) to spectral data (blue bars). In theory, the strength of oscillations (amplitude/noise, T) is determined by the chemoreflex stability. Patients i-ii exhibited strong yet irregular overshoot-undershoot ventilatory oscillations. Patient iii exhibited modest oscillations following a transient disturbance (sigh breaths). Patient iv exhibited strong yet periodic oscillations consistent with instability (loop gain near 1). To the eye, patient v exhibited no overt oscillatory behavior in (**A**), but spectral analysis reveals a weak oscillation (**B**). Amplitude in the scaling bar represents ventilation (tidal volume × respiratory rate).

Figure 4. Reduced chemoreflex stability explains ventilatory oscillations in patients with heart failure. With increasing loop gain, oscillations became stronger relative to biological noise (**A**), larger in amplitude (**B**) and more regular (**C**). (**A**) Notably, the strength of oscillations (spectral height relative to background noise, T) closely matched that predicted from the loop gain of the chemoreflex system regulating ventilation (solid black line, Equation 1). Accordingly the estimated loop gain from the spectra closely matched the measured loop gain (error=0.03±0.09, mean±S.D.). Shading in (**C**) denotes 95% prediction interval of simulated data. Solid circles denote heart failure and open circles denote controls. Patients i-v from Fig. 2 are denoted.

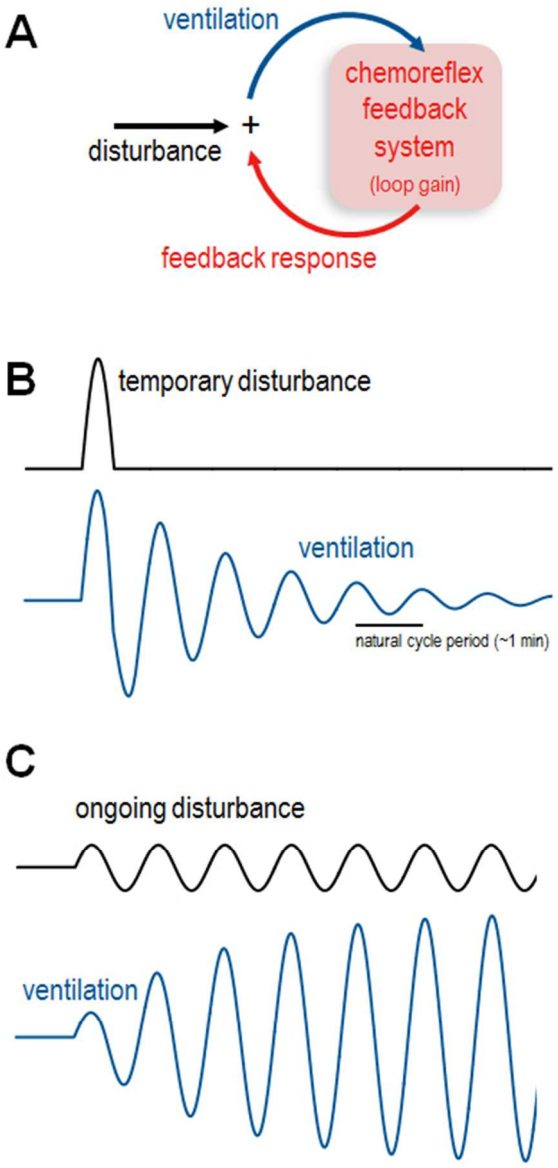

Figure 1. Concept of chemoreflex resonance and the relationship with loop gain. (A) Feedback model for the chemoreflex regulation of ventilation. (B) In a stable system, a temporary disturbance that raises ventilation—thereby lowering alveolar CO2 and later eliciting a reflex reduction in ventilatory drive—ultimately yields a resonance or "ringing" effect characterized by successive overshoot/undershoot fluctuations that damp out over time. Note that each feedback response (overshoot/undershoot) is ~0.8 times smaller than the prior deflection in ventilation (loop gain = 0.8). (C) In the same system, an ongoing disturbance is amplified to yield 5-fold swings in ventilation even though feedback is stable (T=5, see Equation 1).

Figure 1
107x221mm (96 x 96 DPI)

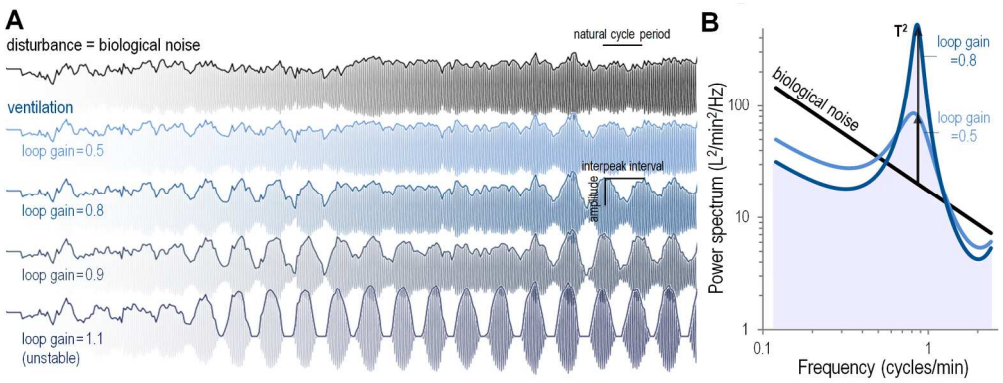

Figure 2. Simulated chemoreflex oscillations. (A) A biological disturbance (top signal) is applied to ventilation for chemoreflex systems with increasing loop gain (reduced stability). Tidal breaths are drawn to faciliate comparison with ventilatory oscillations seen in patients with heart failure. (B) Spectral view of signals in panel A illustrates how biological noise is amplified by the system in a particular range of frequencies (near 1 cycle/min). In theory, the strength of the oscillation (T = amplitude / noise, vertical arrows) at the frequency of periodic breathing ("natural" cycle frequency), is determined by loop gain (Equation 1). Note also that slower disturbances are inhibited (reduced power at lower frequencies) as expected of homeostatic feedback (see Online Supplement).

Figure 2
551x209mm (96 x 96 DPI)

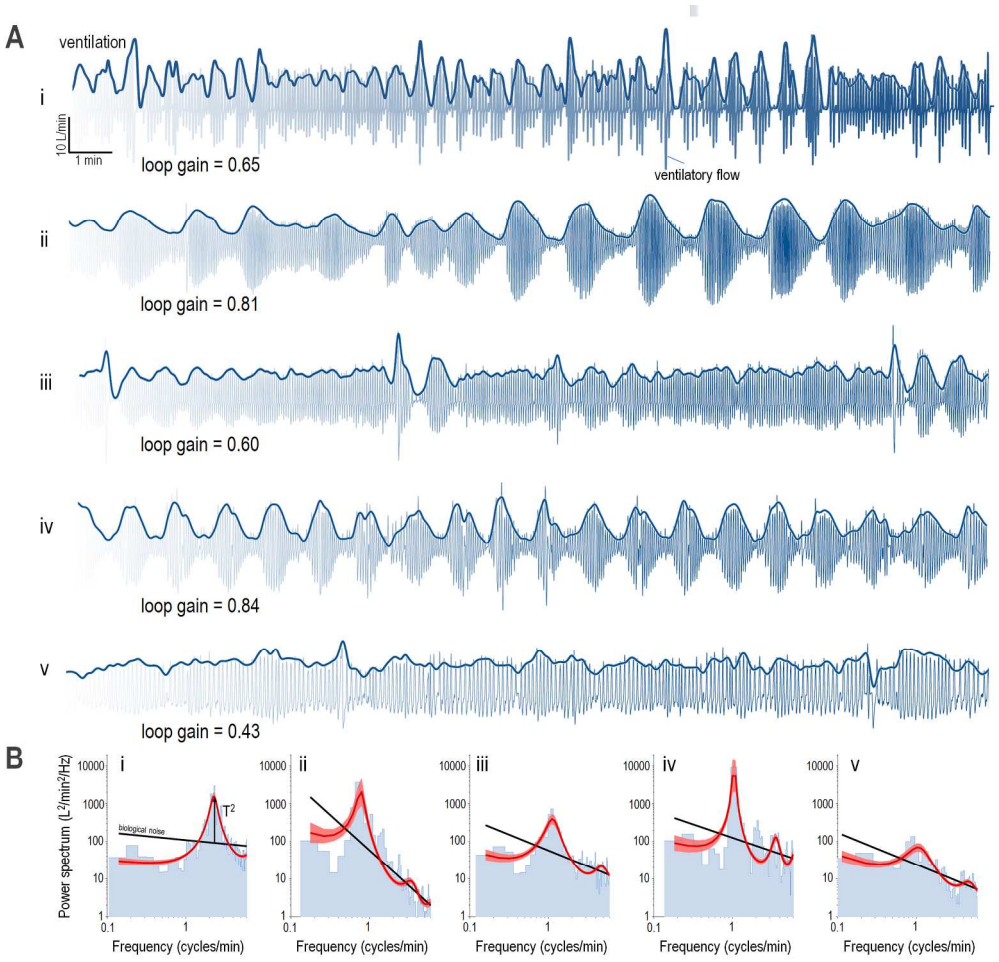

Figure 3. Daytime ventilatory oscillations in patients with heart failure. (A) Ventilation data from 5 patients (i-v) are shown superimposed on ventilatory flow waveforms. (B) Corresponding power spectra are shown. Note the close fit of the resonance model (red lines, shading denotes S.E.M.) to spectral data (blue bars). In theory, the strength of oscillations (amplitude/noise, T) is determined by the chemoreflex stability. Patients i-ii exhibited strong yet irregular overshoot-undershoot ventilatory oscillations. Patient iii exhibited modest oscillations following a transient disturbance (sigh breaths). Patient iv exhibited strong yet periodic oscillations consistent with instability (loop gain near 1). To the eye, patient v exhibited no overt oscillatory behavior in (A), but spectral analysis reveals a weak oscillation (B). Amplitude in the scaling bar represents ventilation (tidal volume × respiratory rate).

Figure 3
629x607mm (96 x 96 DPI)

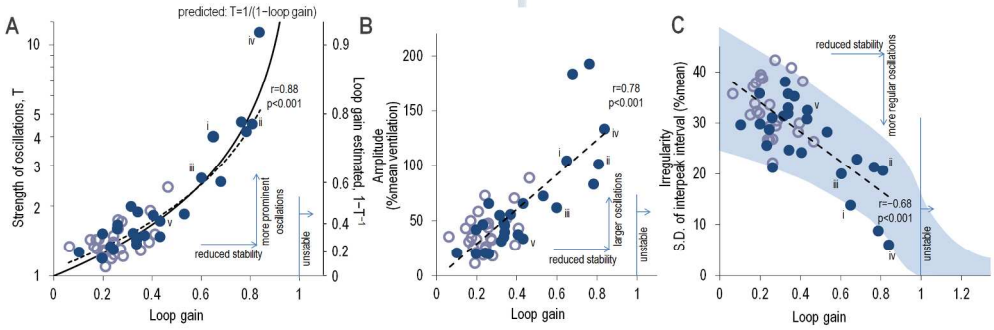

Figure 4. Reduced chemoreflex stability explains ventilatory oscillations in patients with heart failure. With increasing loop gain, oscillations became stronger relative to biological noise (A), larger in amplitude (B) and more regular (C). (A) Notably, the strength of oscillations (spectral height relative to background noise, T) closely matched that predicted from the loop gain of the chemoreflex system regulating ventilation (solid black line, Equation 1). Accordingly the estimated loop gain from the spectra closely matched the measured loop gain (error=0.03±0.09, mean±S.D.). Shading in (C) denotes 95% prediction interval of simulated data. Solid circles denote heart failure and open circles denote controls. Patients i-v from Fig. 2 are denoted.

Figure 4
630x211mm (96 x 96 DPI)

Online Supplement

Resonance as the Mechanism of Daytime Periodic Breathing in Patients with Heart Failure

Scott Sands*, Yoseph Mebrate, Bradley Edwards, Shamim Nemati, Charlotte Manisty, Akshay Desai, Andrew Wellman, Keith Willson, Darrel Francis, James Butler, Atul Malhotra

*Corresponding author. e-mail: sasands@partners.org

The following supplemental data are provided:

METHODS

Background on Instability and Resonance

Instability. The stability of chemoreflex feedback loop controlling ventilation is determined by its *loop gain,* the ratio of the compensatory ventilatory response that opposes a ventilatory disturbance (see conceptual model, Fig. 1A main manuscript)*.

Consider the feedback response to a sinusoidal change in ventilation: If the change in ventilation occurs slowly, the ventilatory response will oppose the sinusoidal deflection (Fig. E1A). At a higher frequency—consequent to the circulation delay—the feedback response will arrive counter-effectively *in phase* with the next deflection in ventilation (Fig. E1B).

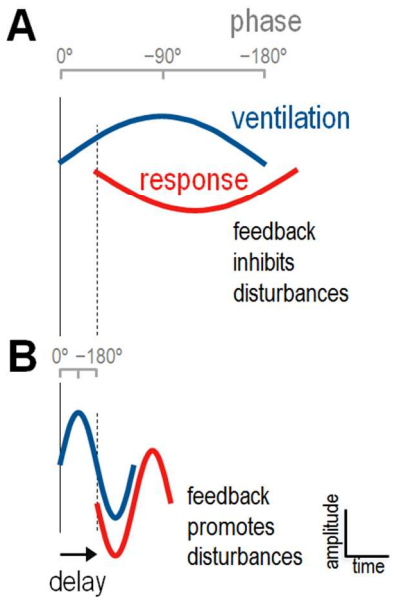

Fig. E1. Feedback promotes oscillations at particular frequencies. Consider a feedback loop with a delay eliciting a feedback response (red) to oppose a ventilatory deflection (blue). (A) For slow disturbances (5 min period, top), the response effectively inhibits the disturbance. (B) For a faster disturbance (1 min period), the same delay causes the feedback response to occur half a cycle too late, acting to promote rather than inhibit the disturbance. The response occurs precisely *in phase* with the disturbance at the system's characteristic *natural frequency*

If, at the characteristic *natural frequency,* the size of the feedback response is smaller than the disturbance (loop gain <1) (Fig. E2A) the system is stable and oscillations will damp out. When loop gain exceeds 1, such that the response is greater than the disturbance, the system is unstable, yielding Cheyne-Stokes respiration (E1-3) (Fig. E2B).

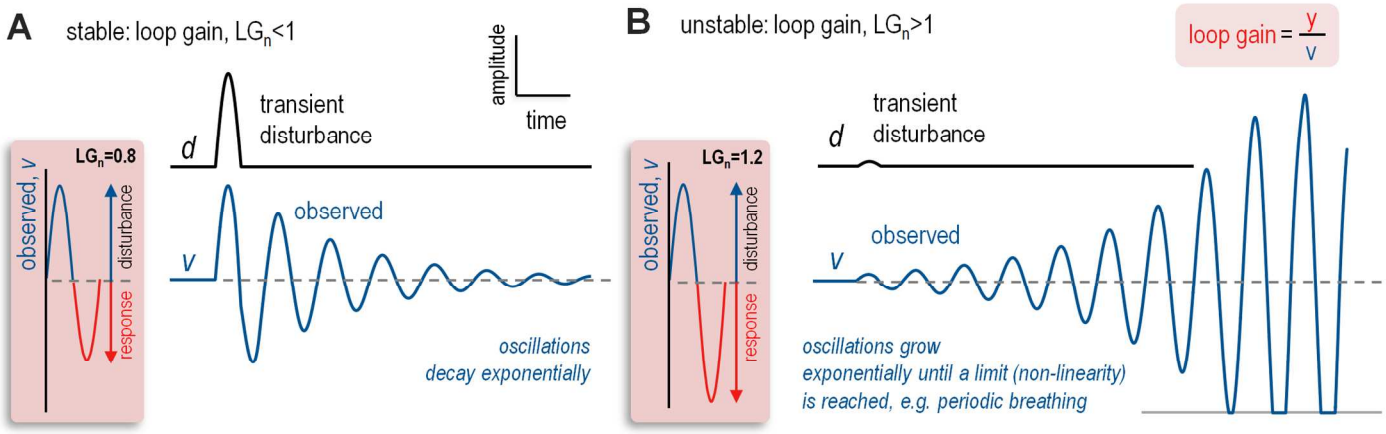

Fig. E2. Feedback instability. The feedback response (red) to a sinusoidal disturbance (blue) at the natural frequency is determined by loop gain (y/v). (**A**) For example, if the response (red line) is smaller than the disturbance (blue line), i.e. loop gain <1, then the system is stable. Note that oscillations which follow a transient disturbance progressively decay. **(B)** If the response is greater than the disturbance, i.e. loop gain >1, then the system is unstable. Hence, a small transient disturbance *d* will result in progressive oscillatory growth until Cheyne-Stokes respiration occurs (see Supplemental Methods—Simulations for details).

**Loop gain* describes the magnitude of the response to a ventilatory disturbance for any given frequency *f*; thus loop gain is formally denoted LG(*f*). LG(*f*) also encapsulates the phase or time lag in the response to a disturbance. At the *natural frequency* f_n the opposing response is half a cycle behind the disturbance. Loop gain at this frequency LG_n determines stability.

Resonance. Now consider the feedback system acting to oppose an ongoing disturbance such that the observed ventilatory fluctuation is the sum of the disturbance and the feedback response. The size of the resultant swings in ventilation relative to the swings in the underlying disturbance are given by (E4-6):

$$T = 1/|1 - \textit{loop gain}| \qquad \text{(Equation 1)}$$

where T is the *transmissibility* or "chemoreflex amplification"*.

Importantly, T varies considerably with the frequency of the disturbance (Fig. E3A): At frequencies where T<1, disturbances are inhibited by the system to promote homeostasis (E4, E6). However, at frequencies where T>1, disturbances are paradoxically amplified by the system. That is, fluctuations are larger (by factor T) because of the presence of feedback versus its absence. The frequency range where T>1 is defined as a *resonance* (red region, Fig. E3). T, when measured at the natural frequency, indicates the strength of the resonance and the ensuing oscillations.

Linking Loop Gain and Resonance

Here we note explicitly that the same single variable that determines stability—loop gain at the natural frequency—also determines the strength of the resonance T at the natural frequency (E7) when breathing is stable. Consequently, as loop gain rises towards 1, the feedback system more powerfully amplifies disturbances into oscillations (Fig. E3A,B). We also show that this phenomenon is an expected feature of all delayed feedback regulatory systems (see below). On this basis, the strength of the resonance, and in turn loop gain, can be inferred by examining the spectral profile of spontaneous oscillations (see Figs. 2, 3A, 4A).

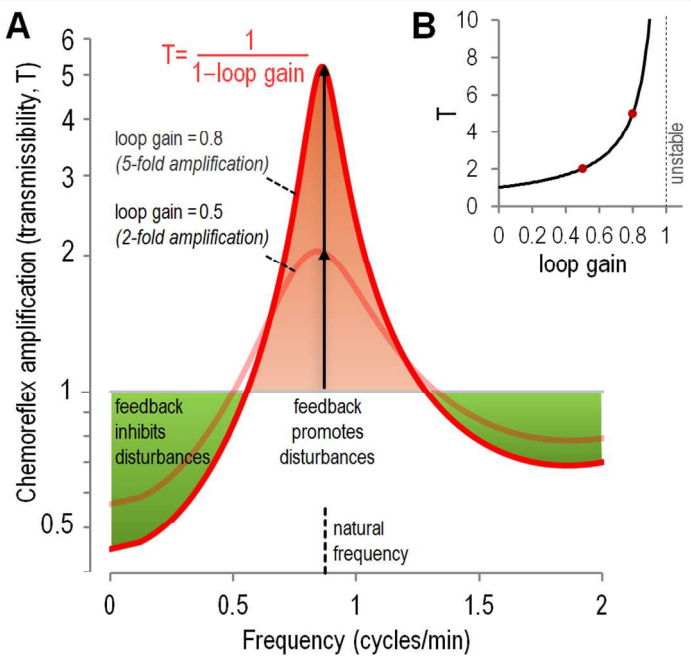

Fig. E3. Chemoreflex amplification versus frequency. (A) Disturbances are suppressed (green) or amplified (red) by the chemoreflex feedback system depending on frequency. The degree of amplification (transmissibility T) reflects the underlying loop gain. For example, a loop gain of 0.5 yields 2-fold amplification (T=2) and a loop gain of 0.8 yields 5-fold amplification (T=5). (B) At the natural frequency, T increases hyperbolically as loop gain approaches 1 (Equation 1) yielding a stronger resonance as the system becomes less stable. Note also, in panel A, that an increased gain improves the inhibition of low frequency (persistent) disturbances at the cost of a stronger resonance. This trade-off is sometimes referred to as the water-bed effect.

*Equation 1 is derived by recognizing that ventilatory deflections v are the sum of the disturbance d and the feedback response y ($v=y+d$), and that the feedback response itself is the result of the system acting on the ventilatory deflection ($y=\mathrm{LG}(f)\times v$) such that $v=\mathrm{LG}(f)\times v+d$. Rearranging to find $\mathrm{T}(f) = |v/d|$ reveals that $\mathrm{T}(f) = 1/|1-\mathrm{LG}(f)|$.

Resonance as an expected feature of all delayed negative feedback systems

Mathematical proof of resonance. To our knowledge, it has not been shown that all feedback systems with a delay must exhibit a resonance (frequency range or ranges with transmissibility>1). Consider a general stable feedback loop X(f) with an additional delay δ, where loop gain is given by $LG(f)=X(f).e^{-i2\pi f\delta}$. This examination reveals that there is always some natural frequency $f=f_n$ at which the phase of the loop ($\varphi_{LG}=\varphi_X-2\pi f\delta \bmod 2\pi$) equals zero. That is, there is no feature of the system X(f)—constrained physically to finite causal functions—that can counteract the linearly decreasing phase of the delay. In the vicinity of the natural frequency (where transmissibility>1 because loop gain [LG_n] is real and positive), disturbances are necessarily amplified despite the system being fundamentally stable ($0<LG_n<1$).

Mathematically, the existence of a natural frequency f_n (at which transmissibility>1) is compulsory when there is some frequency at which the feedback response is in phase with the disturbance at the system input, that is, there is a solution to phase $\varphi_{LG}=0 \pmod{2\pi}$. Consider a general feedback system, denoted X(f), to which we add a delay δ such that the overall feedback system loop gain is given by $LG(f)=X(f)e^{-s\delta}$ (where s is the complex Laplace variable; for frequency analysis $s=i2\pi f$). The phase of this general feedback system is given by $\varphi_{LG}=\varphi_X-2\pi f\delta$. To find a natural frequency f_n, we solve for phase = 0:

$$\varphi_{LG} = \varphi_X - 2\pi f\delta = 0 \pmod{2\pi} \qquad \text{(Equation E1)}$$

The following provides proof that no component of X can provide a phase advance, e.g. negative delay, that can prevent a zero phase crossing without violating causality. If X is a causal system, a sharp signal (e.g. impulse) is applied at the input, the corresponding wave front at the output must occur at or after the time that the impulse occurs; i.e. this response latency or *front delay* of X (δ_X) must not be negative. Equivalently, δ_X can be expressed in terms of the phase φ_x, as:

$$\delta_X = \frac{-1}{2\pi}\lim_{f\to\infty}\frac{d\varphi_X}{df} \geq 0 \qquad \text{(Equation E2)}$$

Eq. E2 illustrates that the phase φ_x can not increase indefinitely at high frequencies without violating causality. Thus, the combination of Eqs. S1 and S2 show that the phase of any system φ_X can not offset the negative phase of the additional delay ($-2\pi f\delta$).

Hence, there will always be at least one frequency at which phase equals zero ($\varphi_{LG}=0$; response is in phase with the disturbance; Eq. E1 is satisfied), such that transmissibility>1 and thus disturbances are paradoxically amplified. The frequency band neighboring this frequency (f_n) describes the region of resonance (transmissibility >1) in which amplification of disturbances necessarily occurs.

The tradeoff between negative feedback suppression and positive feedback amplification (water-bed effect). A necessary consequence of homeostatic feedback (i.e. transmissibility<1 at low frequencies to maintain long term equilibrium) is that more sensitive negative feedback inhibition in one frequency range (transmissibility<1) necessarily yields a greater magnitude of feedback amplification at the resonance/s (transmissibility>1). This inherent trade-off follows from the Bode sensitivity theorem (E8, E9) which states that the fractional increases and decreases in transmissibility about 1 must integrate to zero (note similar areas under and over the curve in Fig. E3).

Mathematically, it can be shown for virtually all delayed feedback systems, that the integral of log(T) across all frequencies (0 to ∞), known as Bode's sensitivity integral, is equal to zero (E8, E9). More generally, for a stable system it can be shown that:

$$\int_0^{\infty} \log_e T \, df = \frac{1}{4} \lim_{s\to\infty}(s \times LG) \qquad \text{(Equation E3)}$$

For the general delayed system $LG=X(f)e^{-s\delta}$, this integral equals zero for any system response $X(f)$ that is bounded at large f (i.e. the feedback response to a high frequency disturbance is not infinite). This is true for all *physically realisable* (finite, real-world) systems such as those governed by differential equations of any finite order, including the first-order delayed system examined here.

Consequently, the existance of a frequency range where disturbances are suppressed (T<1) necessitates that there must be a range where disturbances are amplified (T>1). Quantitatively, the fractional inhibition of disturbances (across all f from 0 to ∞) is precisely offset by the fractional amplification of disturbances at other frequencies. That is, a greater strength of negative feedback, or a broader frequency range of its operation, mathematically necessitates a greater degree (strength or range) of feedback amplification at other (typically higher) frequencies.

Non-linearities. Strictly speaking, the concept of loop gain is most accurately applied in a linear system, or a system that is linearizable with due consideration of important non-linear features. However, we note that in all participants we examined, the linear feedback model captured the essence of the resonance. Moreover, we argue that the existence of non-linearities does not preclude the general expectation that stable feedback regulation will yield resonance and emergent oscillations. For example, feedback incorporating curvi-linearity (e.g. Hill equation (E10)), hysteresis (feedback response to a rising input is shifted relative to the response to a falling input (E11)), more-than-additive or less-than additive interactions can each be shown to exhibit feedback-induced quasi-oscillations similar to those in linear systems.

Simulations

To illustrate feedback amplification conceptually, we employ a simple mathematical model ventilatory control system (one compartment with circulatory delay), in which loop gain is known exactly (Figs. 1, 2, E2-4) (E2, E12). This system has been employed extensively in the analysis of ventilatory control (E1, E2, E12-16) and other systems (E10, E15, E17, E18). The model system used has a loop gain given by $LG(f)=-k/(1+s\tau).e^{-s\delta}$ where k=gain, τ=time constant, δ=delay, $s=i2\pi f$. In the time domain, the behavior of the system is determined by the differential equation $\tau.dy/dt+y=kv(t-\delta)$ where v describes the fluctuations in the controlled variable (i.e. ventilation) and y describes the fluctuations in the feedback response; $v(t)$ and $y(t)$ are functions of time.

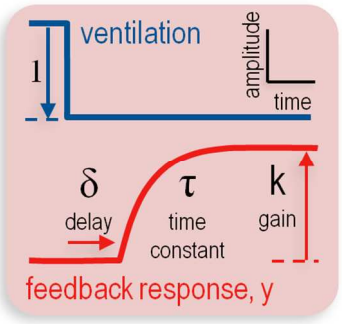

Fig. E4. Simulations were performed using a first-order feedback system (open-loop step-response shown).

Simulations were performed using MATLAB (Mathworks, Natick MA, USA). We employed a ratio of $\delta/\tau = 2$ (25 s delay, 12.5 s time constant) for all simulations to capture the increased circulatory delay in heart failure and approximate the time constant of the lung (E1, E19). Sinusoidal disturbances (Fig. 1C) were provided at the natural frequency of the system (f_n). Biological noise (power law $1/f$ disturbances, Fig. 2A) were simulated by filtering 0.25 Hz white noise (typical 4 s breath duration); S.D.=25% of mean for Fig. 2A. To raise loop gain (at

the natural frequency, LG_n), we increased the feedback gain coefficient (k) which proportionally raises loop gain while maintaining constant natural frequency. Summarized interpeak interval data showing that increased loop gain yields a more regular oscillatory period (Figs. E5 and 4C) was taken from >5000 min of simulations. 95% prediction intervals (Fig. 4C) were based on >500 10-min windows of simulated time-series data (~10 interpeak intervals per window). The analytic solution for the power spectrum of *v* (S_v) was used for Fig. 2B, which matched the mean simulated results.

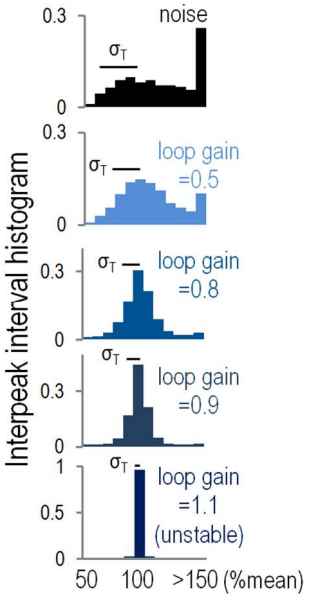

Fig. E5. Interpeak intervals of simulated data. Reduced stability yields a more regular oscillatory period (reduced S.D. of interpeak interval, σ_T).

Terminology

Our use of the term biological noise does not imply the absence of a useful physiological function. The term noise is used to describe the cumulative impact of a host of external or intrinsic sources of stochastic/arrhythmic variability in ventilation.

In contrast to common usage in control systems engineering, we take loop gain, LG(*f*), to be inherently negative at low frequencies. Engineering applications incorporate a separate inverting element which has no biological equivalent. For example, in the ventilatory control system, where loop gain is defined as the product of the controller (Δventilation/ΔPCO_2) and plant (ΔPCO_2/Δventilation), the *plant* is inherently negative at low frequencies (slowly lowering ventilation increases PCO_2). Since the *controller* is inherently positive at low frequencies (slowly increasing PCO_2 increases ventilation), the overall feedback response is inherently negative or inhibitory at low frequencies. Consequences for the formulation of our results versus engineering notation include 1.) the replacement of LG by –LG throughout, and 2.) the definition of the natural frequency as the (lowest) frequency at which phase of LG(*f*) equals 0 rather than −180° (mod 360°).

Data Analysis

To upsample ventilation to 4 Hz we employed the sample-and-hold method. Linear interpolation was used for PCO_2 signals.

Ventilatory Oscillations

To characterize ventilatory oscillations, uninterrupted spontaneous ventilation was measured during supine quiet wakefulness for 20 min. The power spectrum of ventilation was calculated (Welch method, see below) and a resonance model was fit to the ventilation spectrum as follows: Feedback systems disturbed by noise exhibit a spectrum that follows the general form $y=S_d|1-LG(f)|^{-2}$; here we employ the first-order delayed feedback system model in combination with a power-law disturbance given by $S_d=\beta f^{-\alpha}$ (Fig. 2). This resonance model was fit to ventilatory spectra (least squares on logarithmic scale) in the range f=0.1–6 cycles/min (capturing relevant fluctuations between 10 min and 10 s in period). A single parameter, T_n, was taken from the model fit to characterize the oscillatory behavior. Of note, T_n^2, is the spectral peak (at f_n) divided by the background noise. T_n is expected to relate uniquely to loop gain according to Equation 1.

A recognizable feature of quasi-oscillations from the resonance mechanism is the variability of oscillatory timing; truly periodic oscillations should have negligible variability. Oscillations are also expected to become larger as stability is reduced. Hence, we calculated the variability of the interpeak interval; oscillatory peaks in ventilation were located using a subject specific sliding time window of width=$1/f_n$ (0.5±0.2 min; f_n taken from power spectral analysis). Amplitude and phase were identified by finding the best-fit cosine (with fixed frequency f_n) for each windowed data segment using Fourier integration. Peaks were located at the time when phase=0 indicating the presence of a peak in the center of the window. The s.d. of interpeak interval (σ_T) was normalized using the mean interpeak interval (Figs. E5 and 4C). The ventilation time series in Figs 2 and 3 were low-pass filtered for visual presentation of oscillations (cutoff = $4f_n$) but not for spectral analysis.

In the current study we considered that disturbances to ventilatory control were applied to ventilation rather than PCO_2. However, we note that the transmissibility $T(f)$ for ventilation is the same as the transmissibility for PCO_2. Thus, just as for ventilation, resonance effects are expected to transform random changes in PCO_2 (i.e. due to changes in cardiac output) to yield oscillations in PCO_2 depending on loop gain.

Chemoreflex Stability: Summary

To measure the loop gain of the ventilatory control system, $LG(f)$, 0.5-min pulses of 7% inspired CO_2 (in a background of 21% O_2, remainder N_2) were applied every 3 min (Fig. E6). The inspiratory arm of a low-resistance non-rebreathing valve (Hans Rudolph) was connected via inspiratory tubing (22 mm diameter) to a three-way control valve (Hans Rudolph) in an adjacent anteroom allowing the inspiratory line to be switched inconspicuously from room air to a Douglas bag containing the inspired CO_2 (100 L reservoir) at atmospheric pressure. Inspired PCO_2 and end-tidal PCO_2 were measured from the intranasal CO_2 waveform at end-inspiration and end-expiration respectively. All end-tidal PCO_2 data were verified for quality based on the presence of an end-tidal plateau.

In the frequency domain, the CO_2 pulses provided stimulation at 5 frequencies of interest f=1/3, 2/3, 1, 4/3, 5/3 cycles/min. At these frequencies, Fourier transfer analysis yielded estimates of the components of LG: the controller (effect of alveolar PCO_2 swings on ventilation; $C(f) = \Delta V_E$/alveolar PCO_2) and the plant (effect of ventilatory swings on alveolar PCO_2; $P(f) = \Delta$alveolar $PCO_2/\Delta V_E^*$), where $LG(f) = C(f) \times P(f)$. To estimate the characteristics of the plant in the presence of inspired CO_2, changes in the rate of CO_2 excretion at the airway due to the combined effect of inspired PCO_2 and ventilation were expressed as an equivalent fluctuation in ventilation (ΔV_E^*); see below. To characterize the plant, ventilation was corrected for deadspace

([V_T−0.15]/breath duration). To interpolate LG(f) between measured frequencies, models of the controller (delayed, 1-compartment) and plant (2-compartment lung model) were fit to the Fourier transfer-function data for the controller and plant (least squares minimization).

For all frequency-based analyses (power spectral density, transfer ratios, coherence) the Welch method was applied: Data were divided into 4 segments overlapping by 75% and windowed (raised cosine, Hann). Precise frequencies of CO_2 stimulation were identified using the peaks in the inspired PCO_2 power spectra (close to 0.33, 0.67, 1, 1.33, 1.67 cycles/min; Fig. E6D). Frequencies with coherence<0.5 were excluded from analysis.

Causality between the fluctuations in CO_2 and the associated fluctuations in ventilation were confirmed by determining the signal-to-noise ratio for CO_2 and ventilation at each stimulated frequency: The background noise was estimated at frequencies between each harmonic. The signal-to-noise ratios for $PACO_2$ and V_E (at 1 cycle/min, Table S2) were presented to indicate that the majority of the measured oscillatory behavior was attributable to the CO_2 stimulus provided rather than inherent oscillatory behavior.

Chemoreflex Stability: Details

Our modified method to measure the loop gain (LG) of the ventilation-PCO_2 feedback control system combines advantages of previous approaches that utilize inspired CO_2 to measure loop gain and ventilatory stability: pseudo-random binary stimulation (PRBS) and single or multiple-breath (dynamic) CO_2 tests (E20-22). The concept of estimating loop gain using inspired CO_2 is well established (E21, E23-25).

Our approach, like PRBS stimulation, quantifies loop gain by providing dynamic CO_2 stimuli. Mathematical models are then fit to the ventilation and CO_2 data to quantify the plant and controller components of the feedback loop to yield loop gain (controller × plant; see example in Fig. E6A) (E21, E23-25). For the current study, a large signal-to-noise ratio was essential so that the changes in ventilation and PCO_2 due to the stimulation would clearly dominate any possible non-feedback related (i.e. inherent) fluctuations at each frequency of stimulation. Hence, we employed periodic pulses of inspired CO_2 to stimulate the control system at specified frequencies (details below).

By concentrating stimulation and analysis at specified frequencies, we can be confident that the changes in PCO_2 caused the changes to ventilation; that is, the induced changes are large compared with existing background fluctuations. With sufficient stimulation at specified frequencies, the modified method enables determination of the system phase, which is considered unreliable with PRBS (E23). Phase measurement is essential for determining the natural frequency f_n of the system and thus loop gain at this frequency (LG_n).

Theoretical basis. A periodic rectangular pulse waveform (Fig. E2B) can be decomposed into the sum of sinusoids with frequencies f_x and amplitudes a_x given by:

$$f_x = x f_1 \quad \text{and} \quad a_x = \frac{2A}{\pi}\sin(\pi x W f_1) \qquad \text{(Equation E4)}$$

where $1/f_1$ is the period of the pulse waveform, A is the amplitude of the pulse, W is the duration of the pulse (on time), and x denotes the x^{th} frequency component (harmonic). For example, when inspired CO_2 is delivered every $1/f_1$=3 min, the control system becomes stimulated at frequencies of 1/3, 2/3, 1, 4/3, and 5/3 cycles/min. We chose this combination of stimulation to encompass the typical cycling period of ~1 min in patients with

heart failure and periodic breathing (E2, E19, E20, E26, E27). The stimulus duration of W=0.5 min was chosen to maximize the amplitude at 1 cycle/min.

Quantification of plant gain. Here we provide derivation of the equation (Eq. E8) used to calculate the *plant* via Fourier analysis, modified very slightly from Ghazanashah and Khoo (E23) to include second-order effects (interactive effects of changing $PICO_2$ and ventilation). First we re-derive an established relationship describing the plant of the ventilatory control system (E1) using perturbation analysis (Eqs. E5,6), and then confirm that this equation can be recovered in the presence of inspired CO_2 using Eq. E8.

The transport of CO_2 into the lung by the pulmonary circulation and out of the lung by ventilation is given by the following mass balance differential equation (E1, E2, E13, E28):

$$V_L \frac{dPACO_2}{dt} = \dot{Q}\beta(PvCO_2 - PACO_2) - V_E(PACO_2 - PICO_2) \qquad \text{(Equation E5a)}$$

where V_L is lung volume, $\dot{Q}$ is pulmonary blood flow (cardiac output), β describes the capacitance of the blood for CO_2 relative to air, $PvCO_2$ is the partial pressure of CO_2 in the blood entering the lungs via the pulmonary artery, $PACO_2$ is the partial pressure of CO_2 in the lungs. Using perturbation analysis, we break up dynamic variables ($PACO_2$ and V_E) into components reflecting the mean level ($\overline{P}ACO_2$) and the fluctuating component ($\Delta PACO_2$), where $PACO_2 = \overline{P}ACO_2 + \Delta PACO_2$ and $V_E = \overline{V}_E + \Delta V_E$. $PICO_2$ equals zero under normal conditions. Equating the dynamic components, noting that $\Delta V_E \Delta PACO_2$ is negligible for small perturbations, and moving to the frequency domain yields the standard equation for plant gain (E1):

$$P(s) = \frac{\Delta PACO_2}{\Delta V_E} = \overline{P}ACO_2\left[\frac{-1}{V_L(s + 1/\tau)}\right] \qquad \text{(Equation E6)}$$

where $s=i2\pi f$, f is the oscillatory frequency under consideration, $\Delta PACO_2$ and ΔV_E are redefined as frequency domain variables, and the time-constant of the plant is given by $\tau = V_L/(\dot{Q}\beta + \overline{V}_E)$.

Repeating the standard perturbation analysis but now accounting for non-zero inspired CO_2, such that $PICO_2 = \overline{P}ICO_2 + \Delta PICO_2$, and considering that the second-order term $\Delta V_E(\Delta PACO_2 - \Delta PICO_2)$ is no longer negligible (when ventilation and $PICO_2$ fluctuate together during CO_2 stimulation) yields the following expression (contrast with Eq. E6):

$$\frac{\Delta PACO_2}{\Delta V_E(PACO_2 - PICO_2) - \overline{V}_E \Delta PICO_2} = \left[\frac{-1}{V_L(s + 1/\tau)}\right] \qquad \text{(Equation E7)}$$

Finally the plant is recovered by multiplying both sides by $\overline{P}ACO_2^{resting}$ to yield:

$$P(s) = \frac{\Delta PACO_2}{\Delta V_E^*}$$

where

$$\Delta V_E^* = \Delta V_E \frac{PACO_2 - PICO_2}{\overline{P}ACO_2^{resting}} - \Delta PICO_2 \frac{\overline{V}_E}{\overline{P}ACO_2^{resting}} \qquad \text{(Equation E8)}$$

Note that ΔV_E^* contains terms that act on ΔV_E as correction factors for the impact of inspired CO_2. Moreover, since Eq. E8 relies only on assumptions regarding CO_2 excretion via the airway, which is directly measured, this relationship does not depend on the specific plant structure. That is, Eq. E8 can be shown to be valid for more complex plant models including the two-compartment lung model used in the current study.

Controller and plant model topology. To determine loop gain at the natural resonant frequency in human subjects, we fit models to the controller and plant data to provide a measure of gain and phase at frequencies between those stimulated. The topologies chosen for the physiological data were:

$$C(s) = \frac{\Delta V_E}{\Delta PACO_2} = (k_1 + k_2 s)\frac{1}{1+s\tau_1}e^{-\delta s} \qquad \text{(Equation E9)}$$

$$P(s) = \frac{\Delta PACO_2}{\Delta V_E^*} = \frac{k_3}{s+1/\tau_2} + \frac{k_4}{s+1/\tau_3} \qquad \text{(Equation E10)}$$

where $s=i2\pi f$. Physiologically, the controller function (Eq. E9) represents a proportional-plus-differential controller located within in a single homogenous compartment (time constant, τ_1) that receives a supply of arterial CO_2 which is delayed by δ relative to PCO_2 at the lung ($PACO_2$). The proportional component (k_1) represents the steady-state hypercapnic ventilatory response; the differential component ($k_2 s$) represents an additional component that captures the ventilatory response to the *rate of rise* in PCO_2; this component greatly improved the fit to the data in 4/50 participants (all heart failure patients) who exhibited a progressively larger controller response at higher versus lower frequencies (also seen in other physiological reflex systems (E29-32)). For the remaining patients, k_2 was negligible and set to 0. The plant function (Eq. E10) represents two parallel compartments, a form commonly used to describe gas exchange in the lung (E33). The use of a two compartment plant was confirmed to be necessary in the far majority of individuals based on the removal of systematic bias in the model residuals compared to a single compartment model (where $k_4=0$).

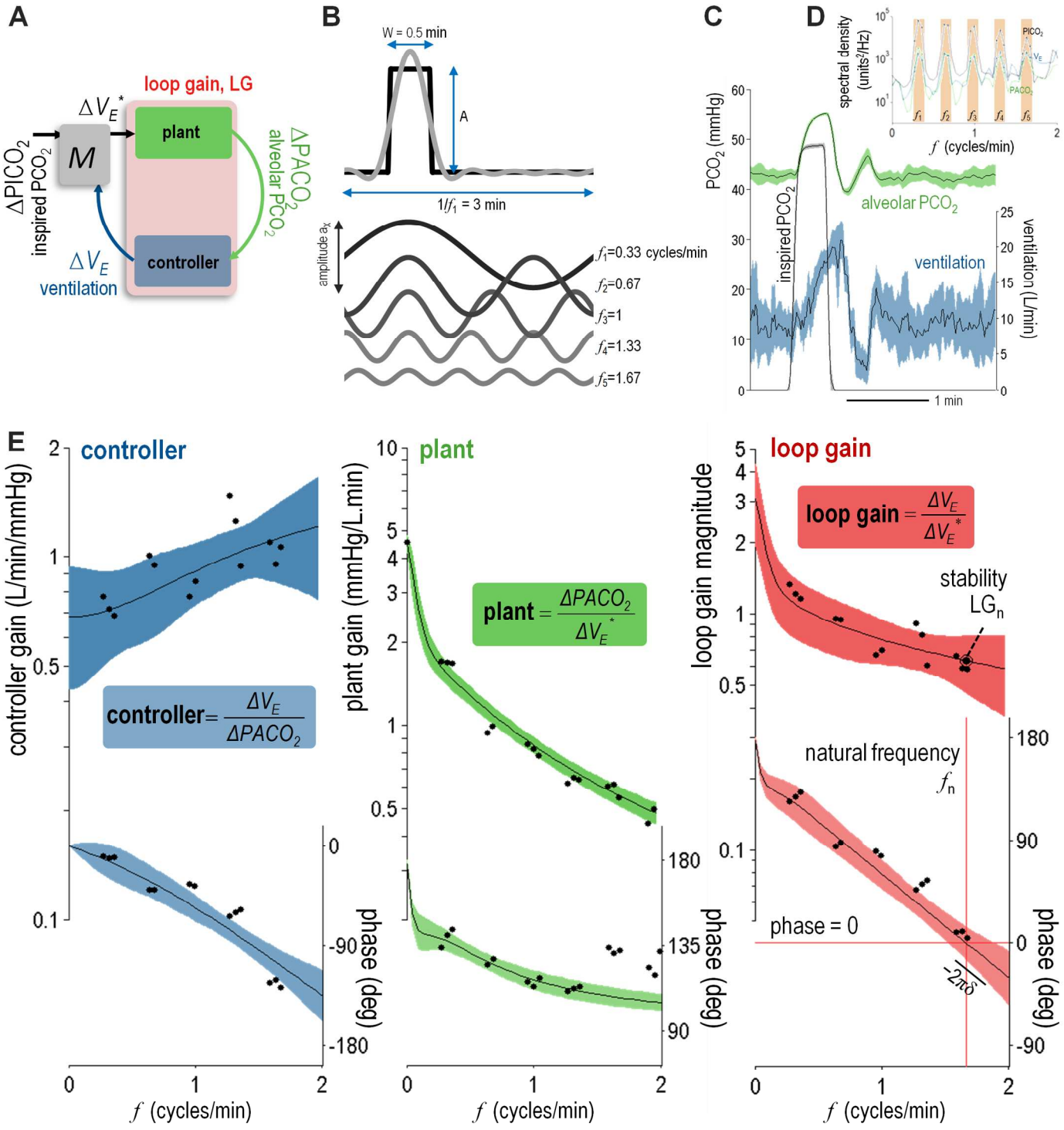

Fig. E6. Measuring ventilatory stability using CO_2 stimulation. (**A**) Schematic of the ventilation–PCO_2 feedback loop illustrating the use of inspired CO_2 to measure the *controller* ($\Delta PACO_2 \rightarrow \Delta V_E$) and the plant ($\Delta V_E^* \rightarrow \Delta PACO_2$, *ventilation corrected for $PICO_2$; M describes how inspired CO_2 acts on the plant, see Eq. E8). (**B**) A rectangular pulse wave of inspired PCO_2 ($PICO_2$) stimulates the feedback system at multiple frequencies (*harmonics*) simultaneously. 5 harmonics are shown (f_1 to f_5) whose sum (grey) is superimposed on the original pulse wave (black). The sinusoidal harmonics of $PICO_2$, $PACO_2$ and V_E are used to measure the magnitude and phase relationships between V_E and $PACO_2$ (*controller* and *plant*) and thus loop gain. (**C** to **E**) Example loop gain data in a patient with heart failure (Patient i in Figs. 3-4). (**C**) Ensemble average time-series of the inspired CO_2 pulses illustrating the impact on $PACO_2$ and V_E. Note the secondary undershoot in $PACO_2$ and V_E that almost yields apnea. (**D**) Spectral density of data in **C** showing the harmonic frequencies (shaded) at which the controller and plant are quantified. (**E**) Controller and plant (magnitude and phase) data. Black lines illustrate the model fit (Eqs. E9-10) to the empirical data (dots). Loop gain is the product of the controller and plant. The natural frequency f_n is the frequency f at which phase = 0. LG_n is the value of loop gain at f_n. The circulatory latency δ is proportional to the slope of the phase plot at high f. Shading in **C** and **E** denote 95%CI.

RESULTS

Ventilatory Oscillations

The presence of a resonance (T>0, model fit to power spectra) became more convincingly significant with increased loop gain (p-values, log-transformed for normality, were inversely associated with loop gain measured with CO_2 stimulation; r=−0.53, p<0.001). The resonance was significant (p<0.05 Fisher F-test) in all individuals with loop gain>0.4 (N=11/11 heart failure, 3/3 controls). Participants without a significant resonance (ventilatory variability resembled noise) tended to have a lower loop gain than those with a significant resonance (0.24±0.05 vs 0.36±0.20, p=0.002).

Determinants of Ventilatory Oscillations

Oscillatory amplitude was associated with increased chemoreflex sensitivity (univariate r^2=0.55, p<0.001) and circulatory delay (univariate r^2=0.06; multiple regression Δr^2=0.14, p<0.001). The irregularity of oscillatory timing (S.D. of interpeak interval) was inversely associated with chemoreflex sensitivity (univariate r^2=0.16, p=0.006), circulatory delay (univariate r^2=0.08, p=0.048; multiple regression Δr^2=0.12, p=0.005), and plant gain (univariate r^2<0.01; multiple regression Δr^2=0.06, p=0.049). Including presence/absence of heart failure did not improve these associations, suggesting that no factor relating to heart failure beyond the determinants reported was associated with ventilatory oscillations.

Inclusion of age, sex and BMI in linear regression models did not impact the statistical findings, and these factors did not significantly contribute to the oscillatory nature of breathing (strength, amplitude, timing).

Reduced versus Preserved Ejection Fraction

Excluding the two patients with heart failure and preserved ejection fraction (HFpEF) also had no impact on the statistical findings. Aside from their ejection fractions, the two patients with HFpEF did not appear to have particularly unusual ventilatory control parameters with respect to the remainder of the heart failure group: They were ranked 8/25 and 23/25 in terms of delay, 9/25 and 2/25 for chemosensitivity, and 7/25 and 10/25 in terms of loop gain (instability). Note that one of the two HFpEF patients had a relatively normal delay (rank 23/25) but a more severely elevated chemosensitivity (rank 2/25) ultimately culminating in a higher-than-average loop gain (rank 10/25). The specific mechanisms involved in the increased chemosensitivity and delays are likely to be different in HFpEF versus heart failure with reduced ejection fraction (e.g. left atrial distension rather than left ventricular distension). However, in principle, increased loop gain (via increased chemosensitivity and delay) is a common physiological pathway to instability applicable to patients with reduced ejection fraction and those with HFpEF.

Sensitivity Analyses

For measurement of the inter-peak interval S.D. (σ_T), alternative use of a fixed window width for the population of between 1–2 cycles/min did not affect the relationship between σ_T and loop gain. Use of a spectral model based on a second-order delayed feedback system $LG(f)=-ke^{-s\delta}/(1+s\tau_1)/(1+s\tau_2)$ did not affect the relationship between the strength of oscillations T (spectral analysis) and true loop gain. In those with large oscillations a minor improvement in the fit using the second order model could be seen. Results of regression analyses

examining the determinants of ventilatory oscillations were similar when exclusively patients with heart failure were examined.

Matched Comparisons between Heart Failure and Controls

We observed several differences in patients with heart failure versus controls including increased loop gain, lower natural frequency and greater chemoreflex delay (Table 2), as well as a greater strength, amplitude and irregularity of ventilatory oscillations (Table 3). These differences remained significant after adjusting for age, sex and BMI (general linear model).

As an alternative to linear adjustment, we repeated group comparisons using a subset of controls (N=16) that were better matched to patients with heart failure for age (controls versus heart failure: 58.3±10.9 vs. 61.1±13.2 years, p>0.4), sex (13M:4F vs 23M:2F, p>0.2), and BMI (30.5±3.3 vs 30.9±7.4 kg/m^2, p>0.8). To make up the subset of matched controls, the youngest 6 women and the youngest 2 men were excluded from the original control group (15M:10F). We found that all statistical differences remained between heart failure and controls for loop gain (p=0.004), natural frequency (p=0.001), chemoreflex delay (p=0.004), and the strength (p=0.004), amplitude (p=0.047) and irregularity (p=0.01) of ventilatory oscillations. Mean values in the control group remained unchanged (<5% vs whole group) for each variable.

More stringent matching on sex (by excluding all female controls except the oldest, 13M:1F vs 23M:2F, p>0.9) also provided similar statistical results (e.g. loop gain: p=0.004, strength of oscillations: p=0.004), although the difference in the amplitude of ventilatory oscillations became non-significant (p=0.08; mean difference remained unchanged) consequent to the reduced statistical power.

Table E1: Data Quality Metrics for Chemoreflex Stability

Characteristics	Heart failure N=25	Controls N=25
Number of Inspired CO_2 Pulses	10±2	10±2
$PACO_2$ Signal-to-noise ratio	52[51]	35[58]
Ventilation Signal-to-noise ratio	12[15]	12[16]
Chemoreflex Coherence ($PACO_2$→ventilation)	0.91±0.08	0.87±0.13
Plant Coherence (ventilation*→$PACO_2$)	0.98±0.02	0.97±0.04

Values are presented as mean±S.D. or median[75th minus 25th percentile]. Signal-to-noise ratio and coherence data are presented for 1 cycle/min. These data indicate that the far majority of the fluctuations observed were caused by the administration of dynamic inspired CO_2. Signal-to-noise is the power spectral density measured at 1 cycle/min relative to the background noise, where background noise is estimated from the nadir power immediately above and below 1 cycle/min (typically at 0.83 and 1.17 cycles/min). Coherence is a value ranging from 0 to 1 that represents the fractional contribution of the input to the output, and is analogous to the R^2. Ventilation* represents the combined effect of ventilation and inspired CO_2 on alveolar PCO_2 ($PACO_2$).

Table E2: Additional Data for Ventilatory Oscillations

Characteristics	Heart failure N=25	Controls N=25
System parameters*		
Gain, k (unitless)	1.7±1.3	1.5±1.2
Time constant, τ (min)	0.34±0.23	0.35±0.28
Delay, δ (min)	0.20±0.07	0.13±0.05*†
Noise characteristics		
Offset, β ($L^2/min^2/Hz$)	2.0[0.8-13.9]	1.2[0.4-6.4]
Exponent, α	0.7±0.4‡	0.7±0.3‡
Data quality		
Duration of recording (min)	20±5	19±6
Goodness of fit‖, r^2	0.56±0.17	0.49±0.16

Values are mean±S.D. or median[25th-75th percentile]. *Chemoreflex resonance model equation is given by $y=S_d(f)/|1-LG(f)|^2$ where $S_d(f)=\beta f^{-\alpha}$ and $LG(f)=-ke^{-i2\pi f\delta}/(1+i2\pi f\tau)$; $S_d(f)$ describes the disturbance (noise) and $LG(f)$ describes the feedback system. †$p<0.001$. ‡The power law exponent was significantly greater than zero (gaussian or white noise) for both groups ($p<10^{-8}$) indicating that disturbances increase in amplitude with lower frequency. ‖Goodness of fit was measured on a logarithmic scale.

MATLAB Source Code: Resonance Model to Estimate Loop Gain

```
function [LGfromPSDdata,Sv,F,Sd_model,Sv_model,CIdata,CIparameters] =
LGfromPSD_beta(v1,dT,order,plotf,Tnmin,Tnmax,Fmin,Fmax)

%Provides power spectral analysis of a time series (for example ventilation) and decomposes the spectrum into
%a biological noise component [Sd_model], and
%a feedback system component (first or second order delayed system)
%where Sv_model=|T|^2.Sd_model and T=1/(1-LG).

%INPUTS
%v1=equispaced time series (e.g. minute ventilation)
%dT=sampling interval
%order is 1 or 2; use 1 by default
%plotf is a flag to show figures
%Tnmin and Tnmax place contraints on min and max cycle period (seconds), use 20 and 90 as defaults.
%min frequency for model fit, specified in Hz, use 1/600 as default.
%max frequency for model fit, specified in Hz, use 1/10 as default.

%OUTPUTS
%LGfromPSDdata = [LGnmodel Tnmodel gain tau1 delay beta alpha tau2 Rsq], describes model parameters
%Sv is power spectral density (PSD)
%F is frequency
%Sv_model is the model PSD that is best fit to Sv
%Sd_model is the 1/f noise component of the model PSD
%CIdata,CIparameters describe the confidence intervals of the model fit and parameters

% Version: Beta
%
% ---------------------------------------------
% Scott A. Sands Ph.D
%
% Sleep Disorders Program
% Brigham and Women's Hospital and Harvard Medical School
% Boston, MA  02115
%
% File created: May 5, 2012
% Last updated: July 5, 2016
%
% Copyright © [2012] Scott A. Sands, Brigham and Women's Hospital, Inc.
%
% THE AUTHORS RETAIN ALL RIGHTS TO THIS SOFTWARE. THIS SOFTWARE IS BEING
% MADE AVAILABLE ONLY FOR SCIENTIFIC RESEARCH PURPOSES. THE SOFTWARE SHALL
% NOT BE USED FOR ANY OTHER PURPOSES, AND IS BEING MADE AVAILABLE WITHOUT
% WARRANTY OF ANY KIND, EXPRESSED OR IMPLIED, INCLUDING BUT NOT LIMITED TO
% IMPLIED WARRANTIES OF MERCHANTABILITY AND FITNESS FOR A PARTICULAR PURPOSE.
% THE AUTHORS AND ITS AGENTS SHALL NOT BE LIABLE FOR ANY CLAIMS, LIABILITIES,
% OR LOSSES RELATING TO OR ARISING FROM ANY USE OF THIS SOFTWARE.

T0 = dT*length(v1);
calforplot=60; %plots are in cycles/min, while input data are provided in sec.

clear i j

if 1 %find Sv
    foverlap = 0.75; No_of_windows = 4;
    fr_segment_ideal = 1/(1+(No_of_windows-1)*(1-foverlap)); T0_segment_ideal = fr_segment_ideal*T0;
    nfft = floor(T0_segment_ideal/dT); noverlap= ceil(foverlap*nfft)+1; nwindow = hann(nfft);
    T0_segment = nfft*dT; df = 1/T0_segment;
    [Sv,F] = pwelch(detrend(v1),nwindow,noverlap,nfft,1/dT);
end

%Fmin=1/600; Fmax=1/10; %10 min to 10 sec
Sv(F<Fmin|F>=Fmax)=[];
F(F<Fmin|F>=Fmax)=[];

%% Find best-fit feedback amplification model

%defaults
lower=[1   0.01  0      -0.1  5  2]; %delay, gain, beta (noise coefficient), alpha (noise exponent), tau1, tau2
(used in second order model)
upper=[100 12 1000000   5   45 1000];
start=[10  0.01  Sv(1) 1    20 45];
```

```
if order==1
    lower(6)=[];
    upper(6)=[];
    start(6)=[];
end

x=start;

Sv_data=[F Sv];
LGnmin=0; LGnmax=1;
coninfo=[Tnmin Tnmax LGnmin LGnmax]
OPTIONS = optimset('TolX',1e-17,'TolFun',1e-17,'MaxIter',1e17,'MaxFunEvals',1000,'Algorithm','interior-
point','Display','off');
clear X FVAL
s=j*2*pi*F;
for i=1:2
    start1 = start;
    try
        [X(i,:),FVAL(i),EXITFLAG,OUTPUT] = fmincon(@(x)
LGfromPSD1(x,Sv_data),start1,[],[],[],[],lower,upper,@(x) LGfromPSD1_con(x,Sv_data,coninfo,1),OPTIONS);
        delay=X(i,1); gain=X(i,2); beta=X(i,3); alpha=X(i,4); tau1=X(i,5);
        if length(X(i,:))==6, tau2=X(i,6); else tau2=0; end
        LGvsFmodel_temp=-gain*exp(-delay*s)./(s*tau1+1)./(s*tau2+1);
        LGnmodel=interp1(F,abs(LGvsFmodel_temp),interp1(unwrap(angle(LGvsFmodel_temp)),F,0));
    catch me %this will happen if start values give LGn>1 or Tn outside constraints
        FVAL(i)=Inf;
    end
end
[~,i]=min(FVAL(2:end))
X2=X(i+1,:);
delay=X2(1); gain=X2(2); beta=X2(3); alpha=X2(4); tau1=X2(5);
if length(X2)==6
    tau2=X2(6);
else
    tau2=0;
end
LGvsFmodel=-gain*exp(-delay*s)./(s*tau1+1)./(s*tau2+1);
absT=abs(1./(1-LGvsFmodel)); Sv_model=(beta*F.^-alpha).*absT.^2; Sd_model=(beta.*F.^-alpha);
angle_LG = unwrap(angle(LGvsFmodel));
Fnmodel=interp1(angle_LG,F,0);
LGnmodel=interp1(F,abs(LGvsFmodel),Fnmodel);

%get 95% CI
if 1
parameters=X2;
    clear modelY_ modelY1 modelY2 f_ f1 f2 parametersX1 parametersX2
    dX=0.000000001;
    for i=1:length(parameters)
        parametersX1=parameters;
        parametersX2=parameters;
        parametersX1(i)=parameters(i)+dX;
        parametersX2(i)=parameters(i)-dX;
        [modelY_]=LGfromPSD2(parameters,F);
        [modelY1(:,i)]=LGfromPSD2(parametersX1,F);
        [modelY2(:,i)]=LGfromPSD2(parametersX2,F);
        JACOBIAN = (-0.5)*(modelY2-modelY1)/dX;
        RESIDUAL = (modelY_-log10(Sv));
    end
end

[log10modelYout,delta] = nlpredci(@LGfromPSD2,F,parameters,RESIDUAL,'Jacobian',JACOBIAN);
upperSEM = 10.^(log10modelYout+delta/1.96);
lowerSEM = 10.^(log10modelYout-delta/1.96);
modelYout = 10.^log10modelYout;
CIdata=[lowerSEM upperSEM];
CIparameters = nlparci(parameters,RESIDUAL,'jacobian',JACOBIAN);

Err=sum((log(Sv_model)-log(Sv)).^2);
SStot=sum((log(Sv)-mean(log(Sv))).^2);
Rsq=1-Err/SStot;

Tnmodel = 1/Fnmodel;

Sdn=interp1(F,Sd_model,Fnmodel);
```

```
Svn=interp1(F,Sv_model,Fnmodel);

%% Plot
if plotf
    facecolorx=[0.8 0.8 1];
    figure100=figure();
    set(figure100,'Color',[1 1 1],'PaperPosition',[0.25 2.5 8 16]);

hha1=subplot(2,2,1,'Parent',figure100,'TickDir','out','FontName','Arial','XScale','log','YScale','log','XMinorTi
ck','on','XLim',60*[min(F)-df*0.55,max(F)+df/2]);
    box(hha1,'off');
    hold(hha1,'all');
    hh1=bar(60*F,Sv,...
        'FaceColor',facecolorx,...
        'EdgeColor','none',...
        'BaseValue',10^(floor(log10(min(Sv_model)))-1),...
        'ShowBaseline','off',...
        'BarWidth',1);
    plot(60*[Fnmodel Fnmodel],[Sdn Svn],'k:');
    title(['LGn=' num2str(LGnmodel,2) '; Tn=' num2str(Tnmodel,2) '; G=' num2str(gain,3) '; D=' num2str(X2(1),2)
'; tau1,2=' num2str(X2(5),2) ',' num2str(tau2,2)],'FontSize',7);
    xlabel('Frequency (cycles/min)');
    ylabel('Power Spectrum [log scale]');

hha2=subplot(2,2,3,'Parent',figure100,'TickDir','out','FontName','Arial','XScale','linear','YScale','linear','XM
inorTick','on','XLim',60*[min(F)-df*0.55,max(F)+df/2]);
    box(hha2,'off');
    hold(hha2,'all');
    hh3=bar(60*F,Sv,...
        'FaceColor',facecolorx,...
        'EdgeColor','none',...
        'BaseValue',0,...
        'BarWidth',1);
    xlabel('Frequency (cycles/min)');
    ylabel('Power Spectrum');

    axes(hha1);
    hold('on');
    filly=[upperSEM' fliplr(lowerSEM')];
    fillx=[F' fliplr(F')];
    fill1 = fill(fillx*calforplot,filly,[1 0.5 0.5],'linestyle','none');
    hhn=plot(F*calforplot,Sd_model,'parent',hha1,'linewidth',2,'color',[0 0 0]);
    hhx=plot(F*calforplot,Sv_model,'parent',hha1,'linewidth',2,'color',[0.9 0 0]);

    hhx=stairs((F-df/2)*calforplot,Sv,'Parent',hha1,'color',[0.5 0.5 0.9]);
    axes(hha2);
    fill1 = fill(fillx*calforplot,filly,[1 0.5 0.5],'linestyle','none');
    hhn=plot(F*calforplot,Sd_model,'parent',hha2,'linewidth',2,'color',[0 0 0]);
    hhx=plot(F*calforplot,Sv_model,'parent',hha2,'linewidth',2,'color',[0.9 0 0]);

    if 1 %Add T to the plots...

hha3=subplot(2,2,2,'Parent',figure100,'TickDir','out','FontName','Arial','XScale','log','YScale','linear','XMino
rTick','on','XLim',60*[0 2.5]);
        hh5=plot(60*F,(Sv_model./Sd_model).^0.5,'r');
        box(hha3,'off');
        set(hha3,'Color','none','XLim',[0 5]);

        set(hha1,'Position',[0.13 0.58 0.77 0.34]);
        set(hha2,'Position',[0.13 0.11 0.77 0.34]);
        set(hha3,'Position',[0.51 0.30 0.35 0.14]);
        ylabel('T');
        xlabel('Frequency (cycles/min)');
    end
end
%%

LGfromPSDdata=[LGnmodel Tnmodel gain tau1 delay beta alpha tau2 Rsq]

function [SSE,Rsq] = LGfromPSD1(x,Sv_data)
delay=x(1);
gain=x(2);
beta=x(3);
alpha=x(4);
tau1=x(5);
if length(x)==6
```

```
    tau2=x(6);
end
F=Sv_data(:,1);
Sv=Sv_data(:,2);
s=j*2*pi*F;
if length(x)==6
    LGvsFmodel=-gain*exp(-delay*s)./(s*tau1+1)./(s*tau2+1);
else
    LGvsFmodel=-gain*exp(-delay*s)./(s*tau1+1);
end
absT=abs(1./(1-LGvsFmodel));
Svmodel=(beta*F.^-alpha).*absT.^2;
SSE=sum(((log10(Svmodel)-log10(Sv))).^2);
SStot=sum(((log10(Sv)-mean(log10(Svmodel)))).^2);

Rsq=1-SSE/SStot;

function [log10Svmodel] = LGfromPSD2(x,F)
%Reframed function for 95%CI
delay=x(1);
gain=x(2);
beta=x(3);
alpha=x(4);
tau1=x(5);
if length(x)==6
tau2=x(6);
end
s=j*2*pi*F;
if length(x)==6
LGvsFmodel=-gain*exp(-delay*s)./(s*tau1+1)./(s*tau2+1);
else
LGvsFmodel=-gain*exp(-delay*s)./(s*tau1+1);
end
absT=abs(1./(1-LGvsFmodel));
Svmodel=(beta*F.^-alpha).*absT.^2;
log10Svmodel=log10(Svmodel);


function [c,ceq]=LGfromPSD1_con(x,Sv_data,coninfo,enable)
if enable
    delay=x(1);
    gain=x(2);
    tau1=x(5);
    if length(x)==6
        tau2=x(6);
    end
    F=Sv_data(:,1);
    s=j*2*pi*F;
    if length(x)==6
        LGvsFmodel=-gain*exp(-delay*s)./(s*tau1+1)./(s*tau2+1);
        phase=pi-atan(2*pi*tau1*F)-atan(2*pi*tau2*F)-2*pi*delay*F;
    else
        LGvsFmodel=-gain*exp(-delay*s)./(s*tau1+1);
        phase=pi-atan(2*pi*tau1*F)-2*pi*delay*F;
    end
    Fn=interp1(phase,F,0,'linear');
    Tn=1/Fn;
    LGn=interp1(F,abs(LGvsFmodel),Fn,'linear');
    c(1)=coninfo(1)-Tn;
    c(2)=Tn-coninfo(2);
    c(3)=coninfo(3)-LGn;
    c(4)=LGn-coninfo(4);
else
    c=[];
end
ceq=[];
```

REFERENCES

E1. Khoo MC, Kronauer RE, Strohl KP, Slutsky AS. Factors inducing periodic breathing in humans: a general model. *J Appl Physiol* 1982;53:644-659.

E2. Francis DP, Willson K, Davies LC, Coats AJ, Piepoli M. Quantitative general theory for periodic breathing in chronic heart failure and its clinical implications. *Circulation* 2000;102:2214-2221.

E3. Sands SA, Edwards BA, Kee K, Turton A, Skuza EM, Roebuck T, O'Driscoll DM, Hamilton GS, Naughton MT, Berger PJ. Loop gain as a means to predict a positive airway pressure suppression of Cheyne-Stokes respiration in patients with heart failure. *Am J Respir Crit Care Med* 2011;184:1067-1075.

E4. Nemati S, Edwards BA, Sands SA, Berger PJ, Wellman A, Verghese GC, Malhotra A, Butler JP. Model-based characterization of ventilatory stability using spontaneous breathing. *J Appl Physiol* 2011;111:55-67.

E5. Hammer PE, Saul JP. Resonance in a mathematical model of baroreflex control: arterial blood pressure waves accompanying postural stress. *Am J Physiol Regul Integr Comp Physiol* 2005;288:R1637-1648.

E6. Nisbet RM, Gurney WSC. A simple mechanism for population cycles. *Nature* 1976;263:319-320.

E7. Ogata K. Frequency response analysis. In: Robbins T, editor. Modern Control Engineering, 3rd ed. New Jersey: Prentice-Hall, Inc.; 1997. p. 471-608.

E8. Bode H. Network Analysis and Feedback Filter Design. New York, NY: D. Van Nostrand Company; 1945.

E9. Freudenberg J, Looze DP. A sensitivity tradeoff for plants with time delay. *Automatic Control, IEEE Transactions on* 1987;32:99-104.

E10. Mackey MC, Glass L. Oscillation and chaos in physiological control systems. *Science* 1977;197:287-289.

E11. Wilkinson MH, Berger PJ, Blanch N, Brodecky V, Jones CA. Paradoxical effect of oxygen administration on breathing stability following post-hyperventilation apnoea in lambs. *J Physiol* 1997;504:199-209.

E12. Wellman A, Eckert DJ, Jordan AS, Edwards BA, Passaglia CL, Jackson AC, Gautam S, Owens RL, Malhotra A, White DP. A method for measuring and modeling the physiological traits causing obstructive sleep apnea. *J Appl Physiol* 2011;110:1627-1637.

E13. Carley DW, Shannon DC. A minimal mathematical model of human periodic breathing. *J Appl Physiol* 1988;65:1400-1409.

E14. Edwards BA, Sands SA, Eckert DJ, White DP, Butler JP, Owens RL, Malhotra A, Wellman A. Acetazolamide improves loop gain but not the other physiological traits causing obstructive sleep apnoea. *J Physiol* 2012;590:1199-1211.

E15. Jia S, Wang L, Luo C. The Research on Stability of Supply Chain under Variable Delay Based on System Dynamics. In: Renko S, editor. Supply Chain Management - New Perspectives: InTech; 2011. p. 673-694.

E16. Khoo MCK. Nonlinear analysis of physiological control systems. In: Herrick RJ, editor. Physiological control systems Analysis, simulation, and estimation. New Jersey: John Wiley & Sons, Inc.; 2000. p. 229-269.

E17. Vasilakos K, Beuter A. Effects of noise on a delayed visual feedback system. *J Theor Biol* 1993;165:389-407.

E18. Stark L, Sherman PM. A servoanalytic study of consensual pupil reflex to light. *Journal of neurophysiology* 1957;20:17-26.

E19. Hall MJ, Xie A, Rutherford R, Ando S, Floras JS, Bradley TD. Cycle length of periodic breathing in patients with and without heart failure. *Am J Respir Crit Care Med* 1996;154:376-381.

E20. Solin P, Roebuck T, Johns DP, Walters EH, Naughton MT. Peripheral and central ventilatory responses in central sleep apnea with and without congestive heart failure. *Am J Respir Crit Care Med* 2000;162:2194-2200.

E21. Khoo MC, Yang F, Shin JJ, Westbrook PR. Estimation of dynamic chemoresponsiveness in wakefulness and non-rapid-eye-movement sleep. *J Appl Physiol* 1995;78:1052-1064.

E22. McClean PA, Phillipson EA, Martinez D, Zamel N. Single breath of CO2 as a clinical test of the peripheral chemoreflex. *J Appl Physiol* 1988;64:84-89.

E23. Ghazanshahi SD, Khoo MC. Estimation of chemoreflex loop gain using pseudorandom binary CO2 stimulation. *IEEE Trans Biomed Eng* 1997;44:357-366.

E24. Topor ZL, Johannson L, Kasprzyk J, Remmers JE. Dynamic ventilatory response to CO(2) in congestive heart failure patients with and without central sleep apnea. *J Appl Physiol* 2001;91:408-416.

E25. Hudgel DW, Gordon EA, Thanakitcharu S, Bruce EN. Instability of ventilatory control in patients with obstructive sleep apnea. *Am J Respir Crit Care Med* 1998;158:1142-1149.

E26. Tkacova R, Niroumand M, Lorenzi-Filho G, Bradley TD. Overnight shift from obstructive to central apneas in patients with heart failure: role of PCO2 and circulatory delay. *Circulation* 2001;103:238-243.

E27. Naughton M, Benard D, Tam A, Rutherford R, Bradley TD. Role of hyperventilation in the pathogenesis of central sleep apneas in patients with congestive heart failure. *Am Rev Respir Dis* 1993;148:330-338.

E28. Grodins FS, Buell J, Bart AJ. Mathematical analysis and digital simulation of the respiratory control system. *J Appl Physiol* 1967;22:260-276.

E29. Ikeda Y, Kawada T, Sugimachi M, Kawaguchi O, Shishido T, Sato T, Miyano H, Matsuura W, Alexander J, Jr., Sunagawa K. Neural arc of baroreflex optimizes dynamic pressure regulation in achieving both stability and quickness. *Am J Physiol* 1996;271:H882-890.

E30. Zahalak GI, Cannon SC. Predictions of the Existence, Frequency, and Amplitude of Physiological Tremor in Normal Man Based on Measured Frequency-Response Characteristics. *J Biomech Eng* 1983;105:249-257.

E31. Matthews PB. The simple frequency response of human stretch reflexes in which either short- or long-latency components predominate. *J Physiol* 1994;481 (Pt 3):777-798.

E32. Petiot E, Barres C, Chapuis B, Julien C. Frequency response of renal sympathetic nervous activity to aortic depressor nerve stimulation in the anaesthetized rat. *J Physiol* 2001;537:949-959.

E33. Wanner A, Zarzecki S, Atkins N, Zapata A, Sackner MA. Relationship between frequency dependence of lung compliance and distribution of ventilation. *J Clin Invest* 1974;54:1200-1213.

main manuscript, marked-up

Resonance as the Mechanism of ~~Diurnal~~Daytime Periodic Breathing in Patients with Heart Failure

Scott A. Sands[1,2*], Yoseph Mebrate[3,4], Bradley A. Edwards[1,5,6], Shamim Nemati[1], Charlotte H. Manisty[7], Akshay S. Desai[8], Andrew Wellman[1], Keith Willson[3], Darrel P. Francis[3], James P. Butler[1†], Atul Malhotra[1,9†]

[1]Division of Sleep and Circadian Disorders, Brigham and Women's Hospital and Harvard Medical School, Boston, USA;
[2]Department of Allergy, Immunology and Respiratory Medicine and Central Clinical School, The Alfred and Monash University, Melbourne, Australia;
[3]International Center for Circulatory Health, National Heart and Lung Institute, Imperial College London, UK.
[4]Department of Clinical Engineering, Royal Brompton Hospital, London, UK;
[5]Sleep and Circadian Medicine Laboratory, Department of Physiology Monash University, Melbourne, VIC, Australia.
[6]School of Psychological Sciences and Monash Institute of Cognitive and Clinical Neurosciences, Monash University, Melbourne,
[7]Institute of Cardiovascular Sciences, University College London, London UK;
[8]Division of Cardiovascular Medicine, Brigham and Women's Hospital and Harvard Medical School, Boston, USA.
[9]Division of Pulmonary and Critical Care Medicine, University of California San Diego, La Jolla CA, USA.

[†]These authors contributed equally to this work.

[*]Corresponding author: Scott Sands, PhD
Division of Sleep Medicine, Brigham and Women's Hospital,
221 Longwood Ave, Boston 02115, MA, USA.
email: sasands@partners.org | T: +1 8579280341 | F: +1 6177327337

Running title: Mechanism of ~~daytime~~ diurnal periodic breathing

Word count: ~~2931~~3470/3500

Author Contributions. Conception and design: SS, YM, BE, SN, AD, DF, AM. Mathematical framework: SS, SN, JP. Model simulations: SS, YM. Modified approach to assess stability: SS. Data collection and analysis: SS, BE, AW, AM. Drafted the manuscript SS, JB. All authors interpreted data, edited the manuscript for important intellectual content, and approved the final draft.

Support: This study was not supported by industry. Our work was financially supported by the American Heart Association (11POST7360012, 15SDG25890059), National Institute of Health (K24HL093218-01A1, 1R01HL090897-01A2, 5R01HL048531-16, R01HL102321 and P01HL095491), National Health and Medical Research Council of Australia (NHMRC, 1053201), the Menzies Foundation, and the American Thoracic Society Foundation. This work was also supported by Harvard Catalyst (National Center for Research Resources and the National Center for Advancing Translational Sciences, National Institutes of Health Award UL1TR001102). Dr. Sands was also co-investigator on grants from the NHMRC (1038402, 1064163) and NIH (R01HL128658). Dr. Malhotra was PI on NIH R01HL085188, K24HL132105 and co-investigator on R21HL121794, R01HL119201, R01HL081823. As an Officer of the American Thoracic Society, Dr. Malhotra relinquished all outside personal income since 2012. ResMed, Inc. provided a philanthropic donation to the UC San Diego in support of a UCSD sleep center. Dr. Desai reported unrelated grants and personal fees from Novartis, personal fees from St. Jude Medical, Merck, Relypsa, and Janssen. The authors declare no competing financial interests.

Formatted: Font: 11 pt
Formatted: Font: Bold
Formatted: Font: 11 pt, Not Bold

main manuscript, marked-up

Formatted: Space After: 3 pt

At a Glance Commentary

Scientific Knowledge on the Subject: Oscillatory breathing during wakefulness predicts mortality in patients with heart failure but the responsible mechanism is unclear. Associations with increased chemosensitivity and circulatory delay suggest instability of the chemoreflex feedback loop, but oscillatory patterns are often irregular which illustrates that our knowledge is incomplete.

What This Study Adds to the Field: Our study provides the mechanism of ~~diurnal~~daytime ventilatory oscillations in heart failure: Ventilatory oscillations occur due to a chemoreflex resonance or "ringing" effect, whereby a reduced stability (increased loop gain)—due to increased chemosensitivity and delay—paradoxically enhances ~~leads to paradoxical amplification of~~ biological noise as it is propagated around the feedback loop, yielding stronger ~~, larger~~ and more regular oscillations as stability is reduced. Our work may facilitate clinical measurement and interpretation of the oscillatory breathing that precedes sudden death in advanced heart failure.

main manuscript, marked-up

Abstract

Rationale: In patients with chronic heart failure, ~~diurnal~~daytime oscillatory breathing at rest is ~~an ominous sign of~~associated with high ~~high risk of~~ mortality risk. ~~Empirical~~ Experimental evidence, e~~—~~including exaggerated ventilatory responses to carbon dioxide (CO_2) and prolonged circulation time, ~~—~~implicates the ventilatory control system and suggests ~~that~~ feedback instability (loop gain>1) is responsible. However, ~~diurnal~~daytime oscillatory patterns often ~~can~~ appear remarkably irregular versus ~~differ markedly from~~ classical instability (Cheyne-Stokes respiration), suggesting our mechanistic understanding is limited.

Objective: We propose that ~~diurnal~~daytime ventilatory oscillations generally result from ~~manifest consequent to~~ a chemoreflex *resonance*, whereby ~~or "ringing" effect, a mechanism by which~~ spontaneous biological variations in ventilatory drive repeatedly induce temporary and irregular ringing effects. Importantly, the ease with which spontaneous biological variations induce irregular oscillations (resonance "strength") rises profoundly as loop gain rises towards 1. We test this hypothesis through a comparison of mathematical predictions against actual measurements in patients with heart failure and healthy controls. ~~biological disturbances are paradoxically amplified as they propagated around a stable chemoreflex feedback loop (loop gain <1). We test the hypothesis that the magnitude of the resonance T depends uniquely on the system stability (T=1/|1−loop gain|); concordance with theory is taken to support resonance as the mechanism responsible.~~

Methods: In 25 patients with chronic heart failure and 25 controls, we examined spontaneous oscillations in ventilation and separately quantified loop gain using dynamic inspired CO_2 stimulation.

Measurements and Main Results: ~~A clear r~~Resonance was detected ~~observed~~ in 24/25 heart failure patients and 18/25 controls. With ~~reduced stability~~increased loop gain—consequent to increased chemosensitivity and delay—the ~~magnitude~~ strength of spontaneous oscillations ~~resonance~~ increased precipitously as predicted (r=0.88), ~~to~~ yielding larger (r=0.78) and more regular ~~oscillations~~ (interpeak interval S.D. ~~of interpeak interval~~, r=−0.68~~; p<0.001 for all~~) oscillations (p<0.001 for all, both groups combined).

Conclusions: Our study elucidates the mechanism underlying ~~diurnal~~daytime ventilatory oscillations in ~~patients with~~ heart failure, and provides a means to measure and interpret these ~~ventilatory~~ oscillations ~~during wakefulness~~ to reveal the underlying chemoreflex hypersensitivity and reduced stability that foretells mortality in ~~heart failure~~this population.

250/250 words

Keywords

instability | loop gain | Cheyne-Stokes respiration | heart failure | chemosensitivity

Formatted: Space After: 3 pt
Formatted: Font: Bold
Formatted: Not Superscript/ Subscript
Formatted: Font: Bold
Formatted: Font: Not Italic

main manuscript, marked-up

Formatted: Space After: 3 pt

Formatted: Space After: 3 pt

INTRODUCTION

The presence of ~~diurnal~~daytime ventilatory oscillations is a powerful prognostic indicator of mortality in patients with chronic heart failure, independent of ~~cardiac function~~ejection fraction and peak oxygen consumption (1-6), but the underlying pathogenesis remains unclear. The feedback system controlling ventilation is strongly implicated based on evidence that patients with oscillatory ventilation exhibit hypersensitive ventilatory chemoreflexes and increased circulatory delays (5, 7, 8) and evidence that ventilatory oscillations are suppressed by interventions that improve stability (lowered loop gain) namely reducing chemoreflex sensitivity, increasing cardiac output or clamping alveolar carbon dioxide (CO_2) levels (5, 9-13). These findings have led to the prevailing view ~~that~~ that feedback instability is responsible (7, 13-16), rather than a central pacemaker (17, 18). Yet there is a broad spectrum of irregular oscillatory patterns observed in patients during wakefulness, many of which differ substantially from the remarkably consistent ~~-~~periodic cycles of apnea and crescendo-decrescendo hyperpnea (Cheyne-Stokes respiration) manifest during sleep and in computer models of feedback instability (16, 19). Thus, an alternative explanation for ~~diurnal~~daytime ventilatory oscillations is needed.

According to prevailing theory, a hypersensitive and delayed ventilatory feedback system will yield ventilatory oscillations when the critical tipping-point for instability is exceeded (loop gain >1), but when the system is fundamentally stable oscillations should be damped away (loop gain <1, see Methods—Theory and Online Supplement Fig. ~~S1~~E1-2) (7, 14, 16, 20). Yet the instability theory has a critical weakness that precludes its general applicability: Even stable feedback systems (loop gain <1) manifest a *resonance* or "ringing" effect whereby random biological disturbances (e.g. intrinsic neural variability, sighs, and behavioral effects) repeatedly disturb ~~are propagated around~~ the feedback loop, promoting temporary ~~. Consequently, prominent~~ overshoot and undershoot oscillations ~~occur~~ with imprecise timing and amplitude (21-24). We propose that this concept underlies the pathogenesis of ~~diurnal~~daytime ventilatory oscillations in patients with heart failure.

Here we assess whether ventilatory oscillations that occur during wakefulness are the consequence of a resonance in the chemoreflex feedback loop regulating ventilation. First we describe and illustrate the concept of resonance as applicable to ventilatory oscillations. Subsequently, we assess ~~diurnal~~daytime ventilatory oscillations in patients with heart failure and controls to test the hypothesis that the oscillatory behavior depends precisely on the stability (loop gain) of the ventilatory chemoreflex system (see Methods—Theory). Concordance with theory is taken to support chemoreflex resonance as the mechanism responsible. Preliminary data have been presented in abstract form (25).

main manuscript, marked-up

Formatted: Space After: 3 pt

METHODS

Theoretical Basis of Resonance

The concepts of loop gain (i.e. stability) and resonance are well established, but the concept that loop gain precisely determines the strength of the resonance and the ensuing oscillatory nature of breathing under normal (stable) conditions has not been detailed previously. (see Online Supplement for details).

Instability. The stability of the chemoreflex feedback loop is determined by its *loop gain,* the ratio of the compensatory ventilatory feedback response that opposes a ventilatory disturbance (see conceptual model, Fig. 1A). An isolated ventilatory disturbance provided to a stable system (loop gain = 0.8; Fig. 1B) yields a oscillatory "ringing" effect at a particular frequency before gradually damping out. Yet

Resonance. an ongoing disturbance at this frequency) produces ventilatory fluctuations that are considerably larger than the disturbance itself (Fig. 1C). The degree ventilation fluctuates as a result of a disturbance (26-30) is determined by loop gain according to:

$$T = 1/(1-\textit{loop gain}) \qquad \text{(Equation 1)}$$

where T defines the strength of the resonance and the strength of the ensuing oscillations.

As loop gain rises towards 1 (i.e. the threshold for instability), the feedback profoundly amplifies disturbances. For example, for a loop gain of 0.5, disturbances are

Formatted: Space After: 3 pt

doubled by the feedback system (T=2); when loop gain is 0.8, disturbances are 5-fold greater than they would have been without feedback ~~yields 2-fold amplification (T=2, using Equation 1) and a loop gain of 0.8 yields 5-fold amplification~~(T=5, ~~(T=5); see~~ Fig. 1C~~-E~~). ~~A *resonance* is an expected feature of all delayed regulatory systems (see Online Supplement).~~

Simulated ventilatory oscillations. To illustrate the oscillatory characteristics that ~~emerge~~ occur in the presence of spontaneous biological variations or "noise" (31)~~consequent to resonance~~, we examined ~~disturbed~~ a ~~simplified~~ simple model system ~~(Fig. 1C-F) with biological noise (i.e. power inversely proportional to frequency) (31, 32)~~ at various levels of loop gain (Fig. 2). Note the distinct emergence of irregular oscillatory patterns (Fig. 2A) that bare a remarkable resemblance to ventilatory patterns observed in heart failure (13, 32, 33) and controls with experimentally-raised loop gain (34) (~~;~~see Results).

Importantly, we now recognize that ~~A~~as loop gain rises, ~~the system manifests~~ a stronger resonance occurs that can be quantitatively identified as a stronger peak in the power spectrum of ventilation (Fig. 2B), ultimately yielding ~~, recognized~~ larger and more regular oscillations~~as a more pronounced peak in the power spectrum of ventilation (Fig. 2B) and, equivalently, as a greater regularity of oscillatory timing (Fig. 2C)~~.

Methodological Approach

Our primary objective was to test whether oscillatory strength—namely amplitude relative to biological noise (i.e. ~~observed resonance strength,~~ T)—is uniquely related to the loop gain of the ventilatory control system according to Equation 1. Loop gain was measured separately using dynamic inspired CO_2 (see below) during wakefulness. We also assessed whether larger amplitude, more regular oscillations are associated with a higher loop gain, and whether the spectral profile of oscillations matches that expected of a resonance.

Participants

Twenty-five patients with ~~clinically defined~~an established clinical diagnosis of chronic heart failure (any left ventricular ejection fraction) and twenty-five controls without heart failure were studied. Participants attended as part of larger ongoing prospective studies investigating the stabilizing mechanisms of acetazolamide and oxygen and the causes of sleep apnea (interventions were not given before/during this study). Inclusion required the absence of severe comorbidities including lung, kidney and liver diseases. Participants taking medications affecting respiratory control (including opioids, benzodiazepines, barbiturates, acetazolamide, theophylline, indomethacin, pseudoephedrine) were excluded. Participants provided written informed consent and approval was granted by the Partners' Institutional Review Board. Details are provided in the Online Supplement.

main manuscript, marked-up

Formatted: Space After: 3 pt

Procedure

Participants were examined by a physician before study procedures. Measures were made in the morning (7am-12pm) to minimize potential time of day effects. Participants were instrumented with a sealed nasal mask to facilitate measurement of ventilation (heated pneumotachograph and pressure transducer; Hans-Rudolph Model 3700, Kansas City, MO, USA; Validyne Engineering Corp., Model MP45-14-871, Northridge, CA, USA; ventilation = tidal volume × respiratory rate). Absence of mask leak was confirmed by forced expiration against a closed exhalation port. A thin catheter was placed through a port in the mask to measure intranasal CO_2 tension (PCO_2; Vacumetrics Inc., Model 17625, Ventura, CA, USA) enabling assessment of inspired PCO_2 and end-tidal PCO_2 (a surrogate for alveolar and arterial PCO_2). ~~, inspired PCO_2 and end-tidal PCO_2 (surrogate for alveolar PCO_2)~~Electroencephalography (C3-A2, O2-A1) was performed to document wakefulness. P~~. P~~articipants lay supine, ~~maintained wakefulness and nasal breathing.~~ and were instructed to relax, keep their eyes open and mouth closed (confirmed via visual assessment) and watched television as a distraction. Ventilation was recorded without interruption for 20 min to assess spontaneous ventilatory oscillations (see below). Participants were subsequently connected to a non-rebreathing circuit for measurement of their chemoreflex stability (i.e. loop gain) using inspired CO_2. For each procedure, a period of acclimation was provided to ensure ventilation and end-tidal PCO_2 settled to an equilibrium before proceeding. Signals were sampled at 125 Hz (Power 1401 and Spike2, Cambridge Electronic Design Limited, Cambridge, UK); breath-by-breath respiratory signals were resampled at 4 Hz for further analyses.

Formatted: Subscript

Formatted: Not Superscript/ Subscript

Ventilatory ~~oscillations~~Oscillations

To quantify the oscillatory nature of ventilation during spontaneous breathing, we performed ~~standard~~ spectral analysis and fit a physiological equation that describes the spectral profile of a ~~simple~~ resonance (Fig. 2B; one-compartment delayed feedback ~~system~~ stimulated by noise, ~~Fig. 2B,~~ see Online Supplement). This analysis revealed a single parameter, T, a measure of the oscillatory strength ~~of ventilatory oscillations~~ (amplitude / background noise) that is theoretically related to loop gain (Equation 1). The peak-to-peak amplitude and irregularity (interpeak interval S.D.) of ventilatory oscillations were also quantified (see Online Supplement).

Chemoreflex ~~stability~~Stability

Loop gain was quantified using dynamic inspired CO_2 stimulation using a modified method employing pulsatile CO_2 stimuli. 7% inspired CO_2 was administered for a duration of 0.5 min, every 3 min for a total of 30 min (10 pulses) that has the equivalent effect of ~~to~~ stimulat~~e~~ing ventilation at 5 frequencies ~~of interest~~ simultaneously (0.33, 0.67, 1, 1.33, 1.67 cycles/min). Chemosensitivity (Δventilation/Δalveolar PCO_2), CO_2

Formatted: Not Highlight

main manuscript, marked-up

Formatted: Space After: 3 pt

damping or *plant gain* (Δalveolar PCO_2/Δventilation) and accompanying delays were calculated at each frequency to determine loop gain (chemosensivity×plant gain, see Online Supplement).

Statistics

Linear regression assessed the relationship between the oscillatory strength (T, spectral analysis) and the underlying loop gain (CO_2 stimulation). Oscillatory strength was first transformed (1−1/T, reflecting the estimated loop gain) before statistical analysis; transformed data became normally distributed and correlations with putative physiological determinants became linear, as expected by theory. Fisher F-tests compared the resonance model of the power spectrum versus the biological noise model without resonance within individuals; a significant improvement over noise confirmed the presence of a resonance (i.e. T significantly >1). Student's t-tests compared variables between heart failure and controls; general linear models compared variables adjusted for age, sex, and BMI (see Online Supplement for matched comparisons). Determinants of loop gain, including chemoreflex sensitivity and delay, were quantified at a common frequency (1 cycle/min) for regression analyses; multiple regression results were summarized by presenting the improvement in the model r^2 with the inclusion of each determinant in a sequential manner (forward stepwise). Unless specified otherwise, *loop gain* refers to the value at the natural frequency. Statistical significance wa~~i~~s ~~taken~~ accepted at $p<0.05$.

main manuscript, marked-up

Formatted: Space After: 3 pt

RESULTS

Characteristics

Participant characteristics are detailed in Table 1. The heart failure population exhibited a range of severities of left ventricular ~~systolic dysfunction~~ejection fraction (ejection fraction range: 15-67%; two individuals had preserved ~~systolic function~~ejection fraction). All heart failure patients ~~and~~ were on optimal medical therapy per attending cardiologist.

Chemoreflex Stability

Assessment of chemoreflex feedback control of ventilation is detailed in Table 2. Patients with heart failure exhibited stable ventilatory control systems during wakefulness (loop gain range: 0.10-0.84) and exhibited a 71% higher loop gain than controls (p=0.003, adjusted for age, sex, BMI).

Ventilatory Oscillations

Example traces. Ventilatory patterns during spontaneous breathing in 5 patients with heart failure are shown in Fig. 3A. Note the profound, irregular oscillations bear a remarkable resemblance to the ventilatory oscillations emerging from feedback amplification of 1/*f* noise (Fig. 3A versus Fig. 2A).

Resonance model. The resonance model closely fit the measured spectral profile of ventilatory oscillations for each participant (see examples in Fig 3B and summary data in Table 3). The presence of a significant resonance was observed in 24/25 patients with heart failure and 18/25 controls (Fisher F-test, comparing resonance to biological noise without feedback). Participants without a significant resonance (ventilatory variability resembled noise) tended to have a lower loop gain (see Online Supplement).

We observed a notable concordance between the oscillatory strength (T) seen using spectral analysis and the underlying loop gain taken from CO_2 stimulation (Fig. 4A), as expected from theory (Equation 1). That is, the underlying loop gain accurately explains the oscillatory nature of ventilation. Importantly, ~~The~~this association enabled loop gain to be ~~accurately~~ estimated accurately from spontaneous oscillations (estimated loop gain = 1−1/T; Fig. 4A).

Consistent with prediction, increasing loop gain was associated with oscillations that were larger (Fig. 4B) and had less irregular timing (smaller S.D. of interpeak interval, Fig. 4C).

The period of spontaneous oscillations was also associated with the measured natural cycling period (1/[natural frequency] based on CO_2 stimulation, r=0.75, p<0.001) consistent with feedback resonance.

Determinants of Reduced Stability and Oscillations

Linear regression models included the four loop gain determinants shown in Table 2.

main manuscript, marked-up

Formatted: Space After: 3 pt

Determinants of chemoreflex stability. Across all participants, increased loop gain was explained by an increase in chemoreflex sensitivity (univariate r^2=0.42, p<0.001), chemoreflex delay (univariate r^2=0.14; multiple regression Δr^2=0.24, p<0.001), and plant gain (i.e. reduced lung volume; univariate r^2<0.01; multiple regression Δr^2=0.13, p<0.001).

Determinants of ventilatory oscillations. A stronger resonance (T, spectral analysis) was associated with increased chemoreflex sensitivity (univariate r^2=0.36, p<0.001), plant gain (univariate r^2<0.01; multiple regression Δr^2=0.15, p<0.001) and circulatory delay (univariate r^2=0.07; multiple regression Δr^2=0.14, p<0.001). The presence/absence of heart failure explained a minor additional component (Δr^2=0.03, p<0.001) suggesting that factors relating to heart failure beyond the determinants reported had a minor independent impact. Oscillatory amplitude and irregularity were also explained by chemoreflex sensitivity and delays (Online Supplement).

main manuscript, marked-up

Formatted: Space After: 3 pt

DISCUSSION

Our study elucidates the mechanism underlying ~~diurnal~~daytime ventilatory oscillations, a key predictor of mortality in patients with heart failure (1-6). We found that reduced stability (increased loop gain)—consequent to increased chemosensitivity, delay and plant gain—yields stronger oscillations precisely as expected based on the theoretical concept of resonance (Equation 1). Specifically, the chemoreflex feedback system regulating ventilation paradoxically enhances biological noise ~~that perturbs ventilation~~ near the frequency of periodic breathing, to yield ~~a continuum of~~ overshoot and undershoot ventilatory oscillations. These ventilatory oscillations in heart failure are typically irregular (Fig. 3A), and conform to a model of feedback resonance in 96% of patients (Fig. 3B). As loop gain rises towards ~~unity~~1, oscillations become larger and more regular (Figs. 2 and 4), yielding prominent periodic breathing despite ~~stability~~ being classed as a 'stable system' according to classical criteria (loop gain<1). In contrast with current understanding, ~~Thus,~~ the more extreme conditions of feedback instability are therefore not necessary for ventilatory oscillations to occur in heart failure~~, in contrast with current understanding~~ (7, 13-16). Overall, our data are remarkably consistent with chemoreflex resonance as the predominant mechanism responsible. Our work therefore provides the field with a validated framework for interpreting and quantifying the broad range of oscillatory ventilatory behaviors seen commonly in patients with heart failure.

Comparison with Available Evidence

By linking the clinical pattern of ventilatory oscillations to the function of the chemoreflex feedback system that regulates ventilation, we provide a unifying explanation for a host of previous empirical findings. Observational studies consistently demonstrate associations between ~~diurnal~~daytime oscillatory breathing in heart failure and factors that promote a less stable feedback regulation of ventilation, namely increased chemosensitivity and circulatory delay (7, 8, 12). Interventions that diminish feedback act to suppress oscillations, seen as a reduced variability and the disappearance of a peak in the power spectrum of ventilation (5, 9-11, 13). In healthy subjects and animals breathing spontaneously, experimental studies have demonstrated ~~correlated~~ associations between ~~spontaneous~~ ventilatory fluctuations and prior swings in ventilation and PCO_2, which are dependent on intact chemosensitivity ~~(23, 27, 38, 39)~~(22, 26, 35). Modeling studies have also suggested that a stronger chemoreflex response or higher loop gain yields quasi-oscillations in the presence of biological noise (24), although a quantitative relationship between oscillatory behavior and ~~with~~ reduced stability had not been proposed or tested experimentally until now. Taken together with the current study, the available evidence now overwhelmingly implicates chemoreflex feedback regulation in the ventilatory oscillations observed.

Physiological Insights

main manuscript, marked-up

Our study experimentally links the nature of ventilatory oscillations to the underlying structure of the chemoreflex control system regulating ventilation. Several key insights can be drawn from our work:

Based on the concept of resonance, some degree of ventilatory oscillations must occur as a necessary side-effect of homeostatic regulation. Specifically, a greater chemoreflex sensitivity will more completely suppress a long-term or steady-state disturbance to ventilation (e.g. a change in respiratory mechanics or metabolic rate), but will yield a greater amplification of biological noise at its characteristic frequency (see Fig. ~~1~~2B, see also~~ ~~ Online Supplement). The greater circulatory delay that occurs in heart failure will increase the amplification at the resonance, but also moves the resonance to a lower frequency where biological noise is greater~~ ~~(36)~~.

Oscillations result from chemoreflex feedback across a stability-instability continuum. ~~, from~~ Individuals with very low loop gain (e.g. 0<loop gain≤0.25) exhibit a pattern resembling biological noise ~~in those with minimal chemoreflex feedback (low loop gain)~~. Those with normal loop gain (0.25<loop gain≤0.5) exhibit weak ~~, to~~ and irregular oscillations~~.~~ ~~in those with reduced stability~~ Patients with elevated loop gain (0.5<loop gain≤1) manifest stronger and more regular oscillations (~~higher loop gain,~~ Fig. 3). Finally, ~~, to~~ consistent periodic breathing occurs in the most extreme cases when the threshold for instability is breached (loop gain>1).

~~Notably, w~~When loop gain is below 1, the magnitude of biological noise plays a key role in the pathogenesis of oscillatory breathing. For example, patients i and iii have quite similar loop gains but patient i has 2-fold larger oscillations due ~~consequent~~ to increased noise (see Figs. 2 and ~~,~~3)~~.~~. Consequently, ventilatory fluctuations can be larger as a consequence of increased loop gain or increased noise. Thus, two distinct phenotypes of excessive ventilatory variability can be described: those driven largely by hypersensitive chemoreflex feedback (normal biological noise levels) and those with ~~normal chemoreflexes but~~ increased biological noise ~~such as~~i.e. ataxic opioid-induced ventilatory ~~oscillations~~ fluctuations (36) or ventilatory fluctuations in rapid-eye movement sleep (37).

The concept of resonance has important implications for periodic breathing during sleep, known as central sleep apnea, which is also a strong prognostic marker of mortality in heart failure (1). Although sleep diminishes chemosensitivity *per se*, ventilatory oscillations become even more prominent (9). Key contributing factors include changes to state (sleep-wake transitions, arousals) and upper-airway patency (e.g. swings in dilator muscle tone) (38). Insofar as arousals and changes to upper-airway patency are tied to PCO_2, such effects effectively raise loop gain by exacerbating changes in ventilation per change in PCO_2. However, to the extent that arousals and upper airway effects are random, they provide an additional source of biological variability that will act to promote oscillatory breathing with maximum impact in those with elevated loop gain. Diminishing these disturbances with ~~(42)(1)instabilityhudgel~~hypnotics/CPAP can indeed

Formatted: Space After: 3 pt

Formatted: Font: Italic

Formatted: Subscript

Formatted: Not Superscript/ Subscript

Formatted: Subscript

Formatted: Space After: 3 pt

improve central sleep apnea (39). Such disturbances may also explain residual events after loop gain is lowered to stable levels with intervention (40). ~~in(41)(42)~~

The concept also has implications for obstructive sleep apnea, a condition characterized by irregular ventilatory oscillations due to a combination of increased upper airway collapsibility and reduced ventilatory stability (41). Interestingly, reducing loop gain can improve obstructive sleep apnea severity even when the control system is strictly stable before intervention (41), potentially due to damping of chemoreflex resonance effects.

Clinical Implications

In patients with heart failure, increased chemosensitivity and consequent ventilatory oscillations are harbingers of the neurohumoral derangement that ultimately predisposes to mortality (42, 43). On this basis, a simple means to quantify reduced stability, as distinct from increased biological noise, may have clinical utility. Importantly, the current work enables a quantitative identification of the propensity to instability in individual patients from spontaneous breathing, without intervention. We and others have used spontaneous breathing to quantify stability (26, 41, 44, 45), but the use of a single variable to estimate stability without intervention has not been validated to date. Our approach may help 1.) recognize the predisposition to Cheyne-Stokes respiration during wakefulness or sleep, 2.) provide a means to titrate medications or screen those at high risk of sudden cardiac death, 3.) assess the impact of novel therapies designed to reduce chemosensitivity. However, ~~F~~further investigation is warranted.

Limitations

Detailed mechanisms. Our study does not attempt to elucidate the specific chemoreceptors responsible for the ventilatory oscillations observed. Peripheral and central chemoreceptor systems may both contribute to the dynamic response measured with CO_2 stimulation, although available evidence suggests an essential role for the carotid body chemoreceptors in the ventilatory oscillations and mortality in heart failure (46-49). Hypoxic chemosensitivity may also play a role (8), so including it in a measure of loop gain may further improve the associations observed. We also did not seek to elucidate the main source of ventilatory noise. Sources may be either extrinsic (e.g. ~~-~~behavioral inputs, neural variability external to chemoreflex feedback) or intrinsic (e.g. neural variability at the level of respiratory pattern generator or within chemoreceptor circuits in the medulla). The precise details of ventilatory disturbances were not under investigation: the essential point is that biological variability acts to disturb ventilation across a broad frequency range in all individuals.

main manuscript, marked-up

End-tidal PCO_2 as an estimate of alveolar and arterial PCO_2. End-tidal PCO_2 is used ubiquitously in ventilatory control studies of patients with and without heart failure to reflect breath-to-breath changes to alveolar and arterial PCO_2. We note that particular care was taken to ensure a sufficient plateau such that end-tidal PCO_2 reflected alveolar levels (see Online Supplement). Moreover, we excluded patients with lung disease; nonetheless, the difference between end-tidal and arterial PCO_2 may be considerable in some patients with heart failure (e.g. via subclinical pulmonary congestion). We note, however, that a constant discrepancy between these two variables will have no impact on the values of loop gain measured as this calculation depends on relative PCO_2 changes rather than the absolute value.

Non-linearities. The resonance concept employed here can be considered a linear simplification of more general nonlinear behavior. We note that spectral analysis of the oscillation traces revealed subtle higher harmonics at multiples of the natural frequency (i.e. not explained by the linear resonance model) in 3/25 patients with heart failure and 0/25 controls, consistent with the absence of nonlinear effects except in extreme cases (see patients ii and iv in Fig. 3, note smaller peaks not explained by the red model trace; see Online Supplement).

Conclusions

Using a combination of mathematical modeling and direct measurement in patients with heart failure, our study demonstrates that ~~diurnal~~daytime breathing oscillations in heart failure are readily explained by a potent resonance or "ringing" effect due to the chemoreflex feedback system regulating ventilation. Reduced stability—consequent to increased chemosensitivity and delay—leads to a greater amplification and propagation of biological noise around the feedback loop, yielding transient overshoot and undershoot oscillations that become profound as stability is reduced. We may now decipher oscillatory characteristics to more readily detect and interpret the otherwise covert increases in chemoreflex sensitivity that are known to occur with advanced heart failure and foretell mortality.

Formatted: Space After: 3 pt

Formatted: Font: Not Bold

Formatted: Subscript

main manuscript, marked-up

Formatted: Space After: 3 pt

Acknowledgements

The authors are grateful for the technical assistance from Alison Foster, Lauren Hess, Pamela DeYoung and Erik Smales, for the medical assessments performed by Drs. Robert Owens, David McSharry, and Jeremy Beitler, for the facilitation of patient recruitment from Drs. ~~Akshay Desai, James Januzzi,~~ Michael Givertz, James Januzzi, Anju Nohria, William Dec, Garrick Stewart, Eldrin Lewis, Leonard Lilly, Lynne Stevenson and for discussions with Drs. Tilo Winkler and Morgan Mitchell.

Formatted: Space After: 3 pt

References

1. Lanfranchi PA, Braghiroli A, Bosimini E, Mazzuero G, Colombo R, Donner CF, Giannuzzi P. Prognostic value of nocturnal cheyne-stokes respiration in chronic heart failure. *Circulation* 1999;99:1435-1440.
2. Corra U, Pistono M, Mezzani A, Braghiroli A, Giordano A, Lanfranchi P, Bosimini E, Gnemmi M, Giannuzzi P. Sleep and exertional periodic breathing in chronic heart failure: Prognostic importance and interdependence. *Circulation* 2006;113:44-50.
3. Guazzi M, Raimondo R, Vicenzi M, Arena R, Proserpio C, Sarzi Braga S, Pedretti R. Exercise oscillatory ventilation may predict sudden cardiac death in heart failure patients. *J Am Coll Cardiol* 2007;50:299-308.
4. Arena R, Myers J, Abella J, Peberdy MA, Pinkstaff S, Bensimhon D, Chase P, Guazzi M. Prognostic value of timing and duration characteristics of exercise oscillatory ventilation in patients with heart failure. *J Heart Lung Transplant* 2008;27:341-347.
5. Ponikowski P, Anker SD, Chua TP, Francis D, Banasiak W, Poole-Wilson PA, Coats AJ, Piepoli M. Oscillatory breathing patterns during wakefulness in patients with chronic heart failure: Clinical implications and role of augmented peripheral chemosensitivity. *Circulation* 1999;100:2418-2424.
6. Brack T, Thuer I, Clarenbach CF, Senn O, Noll G, Russi EW, Bloch KE. Daytime cheyne-stokes respiration in ambulatory patients with severe congestive heart failure is associated with increased mortality. *Chest* 2007;132:1463-1471.
7. Francis DP, Willson K, Davies LC, Coats AJ, Piepoli M. Quantitative general theory for periodic breathing in chronic heart failure and its clinical implications. *Circulation* 2000;102:2214-2221.
8. Giannoni A, Emdin M, Poletti R, Bramanti F, Prontera C, Piepoli M, Passino C. Clinical significance of chemosensitivity in chronic heart failure: Influence on neurohormonal derangement, cheyne-stokes respiration and arrhythmias. *Clin Sci (Lond)* 2008;114:489-497.
9. Fontana M, Emdin M, Giannoni A, Iudice G, Baruah R, Passino C. Effect of acetazolamide on chemosensitivity, cheyne-stokes respiration, and response to effort in patients with heart failure. *Am J Cardiol* 2011;107:1675-1680.
10. Murphy RM, Shah RV, Malhotra R, Pappagianopoulos PP, Hough SS, Systrom DM, Semigran MJ, Lewis GD. Exercise oscillatory ventilation in systolic heart failure: An indicator of impaired hemodynamic response to exercise. *Circulation* 2011;124:1442-1451.
11. Giannoni A, Baruah R, Willson K, Mebrate Y, Mayet J, Emdin M, Hughes AD, Manisty CH, Francis DP. Real-time dynamic carbon dioxide administration: A novel treatment strategy for stabilization of periodic breathing with potential application to central sleep apnea. *J Am Coll Cardiol* 2010;56:1832-1837.
12. Mortara A, Sleight P, Pinna GD, Maestri R, Capomolla S, Febo O, La Rovere MT, Cobelli F. Association between hemodynamic impairment and cheyne-stokes respiration and periodic breathing in chronic stable congestive heart failure secondary to ischemic or idiopathic dilated cardiomyopathy. *Am J Cardiol* 1999;84:900-904.
13. Pinna GD, Maestri R, Mortara A, La Rovere MT, Fanfulla F, Sleight P. Periodic breathing in heart failure patients: Testing the hypothesis of instability of the chemoreflex loop. *J Appl Physiol* 2000;89:2147-2157.
14. Khoo MC, Kronauer RE, Strohl KP, Slutsky AS. Factors inducing periodic breathing in humans: A general model. *J Appl Physiol* 1982;53:644-659.
15. Cherniack NS, Longobardo GS. Cheyne-stokes breathing. An instability in physiologic control. *N Engl J Med* 1973;288:952-957.
16. Sands SA, Edwards BA, Kee K, Turton A, Skuza EM, Roebuck T, O'Driscoll DM, Hamilton GS, Naughton MT, Berger PJ. Loop gain as a means to predict a positive airway pressure suppression of cheyne-stokes respiration in patients with heart failure. *Am J Respir Crit Care Med* 2011;184:1067-1075.
17. Franklin KA, Sandstrom E, Johansson G, Balfors EM. Hemodynamics, cerebral circulation, and oxygen saturation in cheyne-stokes respiration. *J Appl Physiol* 1997;83:1184-1191.
18. Bartsch S, Haouzi P. Periodic breathing with no heart beat. *Chest* 2013;144:1378-1380.
19. Milhorn HT, Guyton AC. An analog computer analysis of cheyne-stokes breathing. *Journal of Applied Physiology* 1965;20:328-333.
20. Nyquist H. Regeneration theory. *Bell System Technical Journal* 1932;11:126-147.
21. Khoo MCK. Complex dynamics in physiological control systems. In: Herrick RJ, editor. Physiological control systems analysis, simulation, and estimation. New Jersey: John Wiley & Sons, Inc.; 2000. p. 271-308.
22. Van den Aardweg JG, Karemaker JM. Influence of chemoreflexes on respiratory variability in healthy subjects. *Am J Respir Crit Care Med* 2002;165:1041-1047.
23. Modarreszadeh M, Bruce EN. Ventilatory variability induced by spontaneous variations of paco2 in humans. *J Appl Physiol* 1994;76:2765-2775.
24. Khoo MC. Determinants of ventilatory instability and variability. *Respir Physiol* 2000;122:167-182.
25. Sands SA, Nemati S, Mebrate Y, Edwards BA, Manisty CH, Turton A, Wellman A, Willson K, Francis DP, Malhotra A. Ventilatory oscillations in stable control systems as an interaction between external disturbances and feedback stability [abstract]. *SLEEP* 2012;35:A48.
26. Nemati S, Edwards BA, Sands SA, Berger PJ, Wellman A, Verghese GC, Malhotra A, Butler JP. Model-based characterization of ventilatory stability using spontaneous breathing. *J Appl Physiol* 2011;111:55-67.
27. Hammer PE, Saul JP. Resonance in a mathematical model of baroreflex control: Arterial blood pressure waves accompanying postural stress. *Am J Physiol Regul Integr Comp Physiol* 2005;288:R1637-1648.
28. Nisbet RM, Gurney WSC. A simple mechanism for population cycles. *Nature* 1976;263:319-320.
29. Ogata K. Frequency response analysis. In: Robbins T, editor. Modern control engineering, 3rd ed. New Jersey: Prentice-Hall, Inc.; 1997. p. 471-608.
30. Bode H. Network analysis and feedback filter design. New York, NY: D. Van Nostrand Company; 1945.
31. Mutch WA, Harms S, Ruth Graham M, Kowalski SE, Girling LG, Lefevre GR. Biologically variable or naturally noisy mechanical ventilation recruits atelectatic lung. *Am J Respir Crit Care Med* 2000;162:319-323.
32. Garde A, Sornmo L, Jane R, Giraldo BF. Breathing pattern characterization in chronic heart failure patients using the respiratory flow signal. *Ann Biomed Eng* 2010;38:3572-3580.
33. Mortara A, Sleight P, Pinna GD, Maestri R, Prpa A, La Rovere MT, Cobelli F, Tavazzi L. Abnormal awake respiratory patterns are common in chronic heart failure and may prevent evaluation of autonomic tone by measures of heart rate variability. *Circulation* 1997;96:246-252.
34. Wellman A, Malhotra A, Fogel RB, Edwards JK, Schory K, White DP. Respiratory system loop gain in normal men and women measured with proportional-assist ventilation. *J Appl Physiol* 2003;94:205-212.
35. Khatib MF, Oku Y, Bruce EN. Contribution of chemical feedback loops to breath-to-breath variability of tidal volume. *Respir Physiol* 1991;83:115-127.
36. Farney RJ, Walker JM, Cloward TV, Rhondeau S. Sleep-disordered breathing associated with long-term opioid therapy. *Chest* 2003;123:632-639.

Formatted: Space After: 3 pt

37. Rostig S, Kantelhardt JW, Penzel T, Cassel W, Peter JH, Vogelmeier C, Becker HF, Jerrentrup A. Nonrandom variability of respiration during sleep in healthy humans. *Sleep* 2005;28:411-417.
38. Pinna GD, Robbi E, Pizza F, Caporotondi A, La Rovere MT, Maestri R. Sleep-wake fluctuations and respiratory events during cheyne-stokes respiration in patients with heart failure. *J Sleep Res* 2014;23:347-357.
39. Quadri S, Drake C, Hudgel DW. Improvement of idiopathic central sleep apnea with zolpidem. *J Clin Sleep Med* 2009;5:122-129.
40. Sands SA, Edwards BA, Kee K, Stuart-Andrews CR, Skuza EM, Roebuck T, Turton A, Hamilton GS, Naughton MT, Berger PJ. Control theory prediction of resolved cheyne-stokes respiration in heart failure. *European Respiratory Journal* 2016;In Press.
41. Terrill PI, Edwards BA, Nemati S, Butler JP, Owens RL, Eckert DJ, White DP, Malhotra A, Wellman A, Sands SA. Quantifying the ventilatory control contribution to sleep apnoea using polysomnography. *Eur Respir J* 2015;45:408-418.
42. Giannoni A, Emdin M, Bramanti F, Iudice G, Francis DP, Barsotti A, Piepoli M, Passino C. Combined increased chemosensitivity to hypoxia and hypercapnia as a prognosticator in heart failure. *J Am Coll Cardiol* 2009;53:1975-1980.
43. Ponikowski P, Chua TP, Anker SD, Francis DP, Doehner W, Banasiak W, Poole-Wilson PA, Piepoli MF, Coats AJ. Peripheral chemoreceptor hypersensitivity: An ominous sign in patients with chronic heart failure. *Circulation* 2001;104:544-549.
44. Asyali MH, Berry RB, Khoo MC. Assessment of closed-loop ventilatory stability in obstructive sleep apnea. *IEEE Trans Biomed Eng* 2002;49:206-216.
45. Fleming PJ, Goncalves AL, Levine MR, Woollard S. The development of stability of respiration in human infants: Changes in ventilatory responses to spontaneous sighs. *J Physiol* 1984;347:1-16.
46. Khoo MC, Yang F, Shin JJ, Westbrook PR. Estimation of dynamic chemoresponsiveness in wakefulness and non-rapid-eye-movement sleep. *J Appl Physiol* 1995;78:1052-1064.
47. Del Rio R, Marcus NJ, Schultz HD. Carotid chemoreceptor ablation improves survival in heart failure: Rescuing autonomic control of cardiorespiratory function. *J Am Coll Cardiol* 2013;62:2422-2430.
48. Niewinski P, Janczak D, Rucinski A, Jazwiec P, Sobotka PA, Engelman ZJ, Fudim M, Tubek S, Jankowska EA, Banasiak W, Hart EC, Paton JF, Ponikowski P. Carotid body removal for treatment of chronic systolic heart failure. *International journal of cardiology* 2013;168:2506-2509.
49. Solin P, Roebuck T, Johns DP, Walters EH, Naughton MT. Peripheral and central ventilatory responses in central sleep apnea with and without congestive heart failure. *Am J Respir Crit Care Med* 2000;162:2194-2200.
50. Wellman A, Eckert DJ, Jordan AS, Edwards BA, Passaglia CL, Jackson AC, Gautam S, Owens RL, Malhotra A, White DP. A method for measuring and modeling the physiological traits causing obstructive sleep apnea. *J Appl Physiol* 2011;110:1627-1637.

main manuscript, marked-up

Formatted: Space After: 3 pt

TABLES

Table 1: Patient Characteristics

Characteristics	Heart failure N=25	Controls N=25
Male:Female	23:2	15:10†
Age, years	61±13	53±13
Body mass index (kg/m^2)	31±7	32±7
Systolic dysfunction (Y:N)	23:2	-
Left-ventricular ejection fraction (%)	38±15	60±3‡§
New York Heart Association class (I:II:III), N	3:13:8	-
Medications, N (%)		
Beta-blockers	24 (96)	0 (0)†
Loop diuretics	17 (68)	0 (0)†
ACEi or AT2R blockers	23 (92)	2 (8)†
Spironolactone	9 (36)	0 (0)†
Digoxin	6 (24)	0 (0)†

Values are mean±S.D. †p<0.05 (Fisher exact test). ‡Measured in a subset of 5/26 controls (and all participants with heart failure). §p<0.001 heart failure vs. controls (Student's t-test). ACEi=angiotensin-converting enzyme inhibitor. AT2R=angiotensin type II receptor.

Table 2. Chemoreflex stability

Characteristics	Heart failure N=25	Controls N=25
Summary		
Loop gain	0.43±0.21 (range: 0.10-0.84)	0.25±0.09*** (range: 0.06-0.45)
Natural frequency (cycles/min)	1.33±0.39 (range: 0.78-2.57)	1.85±0.51*** (range: 1.15-2.63)
Loop gain determinants‡:		
Chemoreflex sensitivity (L/min/mmHg)§	0.59±0.24	0.48±0.20†
Plant gain (mmHg/L.min)§	0.89±0.21	0.99±0.23
Chemoreflex delay (s)‖	18.2±4.6	13.8±3.3**
Plant delay (s)‖	7.9±1.4	8.2±1.6

Values are mean±S.D. **p<0.01, ***p<0.001 heart failure versus controls. †Non-significant trend (p=0.08). ‡Values are reported for 1 cycle/min oscillations. §Chemoreflex sensitivity or *controller gain* describes the change in ventilation in response to a 1 mmHg oscillation in alveolar PCO_2. Plant gain describes the change in alveolar PCO_2 caused by a 1 L/min oscillation in ventilation. ‖Chemoreflex delay describes the phase shift between alveolar PCO_2 and ventilation (delay = phase lag / 360° × 60) (7). This value reflects the lung-to-chemoreceptor circulation time plus additional time lags due to mixing of CO_2 in the blood and tissues. Likewise, plant delay describes the phase shift between ventilation and alveolar PCO_2 due to CO_2 mixing in the lungs. Values are presented in units of time rather than phase to facilitate interpretation.

main manuscript, marked-up

Formatted: Space After: 3 pt

Table 3. Ventilatory oscillations

Characteristics	Heart failure N=25	Controls N=25
Power spectral analysis of feedback amplification*		
Oscillatory strength, T	1.7 [1.2] (range: 1.2-11.3)	1.4 [0.2]††† (range: 1.1-2.4)
Estimated loop gain, 1−1/T~~−1~~	0.46±0.19	0.29±0.11†††
Estimated natural frequency (cycles/min)	1.7±0.5	2.5±0.6†††
Significant resonance detected‡ (Y:N)	24:1	18:7§
Time-domain analysis		
Amplitude (%mean)	47 [44]	34 [23]†
Inter-peak interval ~~variability,~~ S.D. (%mean)	26±8	33±6††

Values are mean±S.D. or median[75th minus 25th percentile]. *A resonance model was fit to the ventilation power spectrum to summarize the data. The general model is given by $y=S_d(f)/|1-LG(f)|^2$ where the noise component $S_d(f)$ is assumed to conform to a power law ($S_d(f)=\beta f^{-\alpha}$ where α=exponent, β=offset, f=frequency) ~~(50)~~ and the chemoreflex influence is described by the simplest possible model ($LG(f)=-ke^{-i2\pi f\delta}/(1+i2\pi f\tau)$ where k=gain, τ=time-constant, δ=delay) (41, 50). †p<0.05, ††p<0.01, †††p<0.001. ‡Fisher F-test compared the resonance model (feedback stimulated by biological noise) to noise (without feedback) for each individual. §p<0.05 Fisher exact test.

main manuscript, marked-up

Figure Legends

Figure 1. ~~Model~~ Concept of chemoreflex resonance and the relationship with loop gain. (**A**) ~~Conceptual~~ Feedback model ~~of~~ for the chemoreflex ~~feedback~~ regulation of ventilation~~: *v*=variable of interest, *d*=disturbance~~. (**B**) In a stable ~~<I think explain the axes and some more background>~~system, a temporary disturbance that raises ventilation—thereby lowering alveolar CO_2 and later eliciting a reflex reduction in ventilatory drive—ultimately yields a resonance or "ringing" effect characterized by successive overshoot/undershoot fluctuations that damp out over time. Note that each feedback response (overshoot/undershoot) is ~0.8 times smaller than the prior deflection in ventilation (loop gain = 0.8). (**C**) In the same systems, a~~(**B**) Time delays transform feedback inhibition into feedback amplification at higher frequencies: A loop with a delay elicits a response (*red*) to oppose a ventilatory deflection (*blue*). For slow disturbances, the response opposes the disturbance (*top*). For faster disturbances (*bottom*), the delay provides a substantial phase shift; at the natural frequency (phase=0º) disturbances are amplified rather than suppressed. (**C**) Disturbances are suppressed (green) or amplified (red) by the chemoreflex system depending on frequency (Equation 1). The degree of amplification (*transmissibility* T) reflects the underlying loop gain. Amplification profile is shown for a basic feedback system (**D**) that is stable as indicated by the decaying response to a transient disturbance (**E**). (**F**) Despite stability, a~~n ongoing ~~a~~ ongoing sinusoidal ~~disturbance applied at the natural frequency~~ is amplified to yield ~~2-~~fold and 5-fold swings in ventilation even though feedback is stable (T=5, see Equation 1) ~~for loop gains of 0.5 and 0.8 (Equation 1).~~

Figure 2. Simulated chemoreflex oscillations. (**A**) A biological disturbance (~~power inversely related to frequency,~~ top signal) is applied to ventilation for chemoreflex systems with increasing loop gain (reduced stability). Tidal breaths are drawn to faciliate comparison with ventilatory oscillations seen in patients with heart failure. (**B**) Spectral view of signals in panel **A** illustrates ~~ing amplification of~~how biological noise is amplified by the system in a particular range of frequencies (near 1 cycle/min). In ~~principle~~theory, the strength of the oscillation ~~at the natural frequency~~ (T = amplitude / noise, vertical arrows) at the frequency of periodic breathing ("natural" cycle frequency), is determined by loop gain (~~see~~ Equation 1). Note also that slower disturbances are inhibited (reduced power at lower frequencies) as expected of homeostatic feedback (see Online Supplement).~~(**C**) Reduced stability also yields a more regular oscillatory period (reduced S.D. of interpeak interval, σ_L). Simulations were performed using the simplified model in Fig. 1.~~

Figure 3. ~~Diurnal~~Daytime ventilatory oscillations in patients with heart failure. (**A**) Ventilation data from 5 patients (i-v) are shown superimposed on ventilatory flow waveforms. (**B**) Corresponding power spectra are shown. Note the close fit of the resonance model (red lines, shading denotes S.E.M.) to spectral data (blue bars). In theory, the strength of oscillations (amplitude/noise, T) is determined by the chemoreflex stability. Patients i-ii exhibited strong yet irregular overshoot-undershoot ventilatory oscillations. Patient iii ~~exhibits~~ exhibited modest oscillations following a transient disturbance (sigh breaths). Patient iv ~~exhibits~~ exhibited strong yet periodic oscillations consistent with instability (loop gain near 1). To the eye, ~~Patient~~ patient v ~~exhibits~~ exhibited no overt oscillatory behavior in (**A**), but spectral analysis reveals a weak oscillation (**B**). Amplitude in the scaling bar represents ventilation (tidal volume × respiratory rate).

Figure 4. Reduced chemoreflex stability explains ventilatory oscillations in patients with heart failure. With increasing loop gain, oscillations ~~become~~ became stronger relative to biological noise (**A**), larger in amplitude (**B**) and more regular (**C**). (**A**) Notably, the strength of oscillations (spectral height relative to background noise, T) closely ~~matches~~ matched that predicted from the loop gain of the chemoreflex system regulating ventilation (solid black line, Equation 1). Accordingly the estimated loop gain from the spectra closely ~~matches~~ matched the measured loop gain (error=0.03±0.09, mean±S.D.). Shading in (**C**) denotes 95% prediction interval of simulated data. Solid circles denote heart failure and open circles denote controls. Patients i-v from Fig. 2 are denoted.

Formatted: Space After: 3 pt

Formatted: Font: Bold

Formatted: Subscript

Formatted: Font: Bold